nature neuroscience

SUPPLEMENTARY INFORMATION

https://doi.org/10.1038/s41593-017-0004-1

In the format provided by the authors and unedited.

Altered cerebellar connectivity in autism and cerebellar-mediated rescue of autism-related behaviors in mice

Catherine J. Stoodley[1]*, Anila M. D'Mello[1], Jacob Ellegood[2], Vikram Jakkamsetti[3], Pei Liu[3], Mary Beth Nebel[4], Jennifer M. Gibson[3], Elyza Kelly[3], Fantao Meng[3], Christopher A. Cano[3], Juan M. Pascual[3], Stewart H. Mostofsky[4], Jason P. Lerch[2] and Peter T. Tsai[3]*

[1]Department of Psychology and Center for Behavioral Neuroscience, American University, Washington, DC, USA. [2]Toronto Mouse Imaging Centre, Hospital for Sick Kids, Toronto, Canada. [3]The Department of Neurology and Neurotherapeutics, University of Texas Southwestern Medical Center, Dallas, Texas, USA. [4]Center for Neurodevelopmental and Imaging Research, Kennedy Krieger Institute, Baltimore, Maryland, USA. *e-mail: stoodley@american.edu; peter.tsai@utsouthwestern.edu

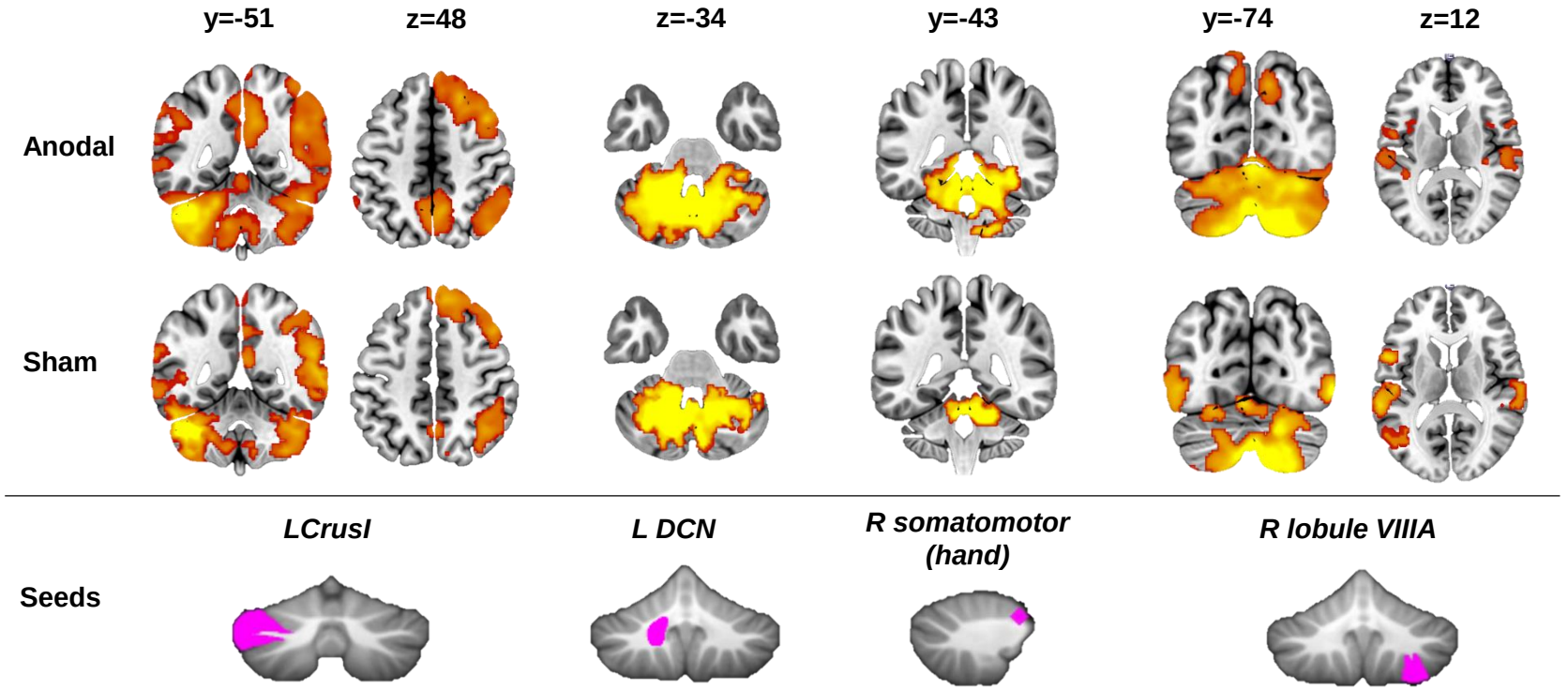

Supplementary Figure S1. Functional connectivity patterns from control seeds in neurotypical adults (LCrusI, L cerebellar nuclei [DCN; dentate nucleus], R cerebellar somatomotor hand area, and R lobule VIIIA) between anodal tDCS (top) and sham treatment (bottom). Voxel-level $p<0.001$, FDR cluster corrected $p<0.05$; n=34.

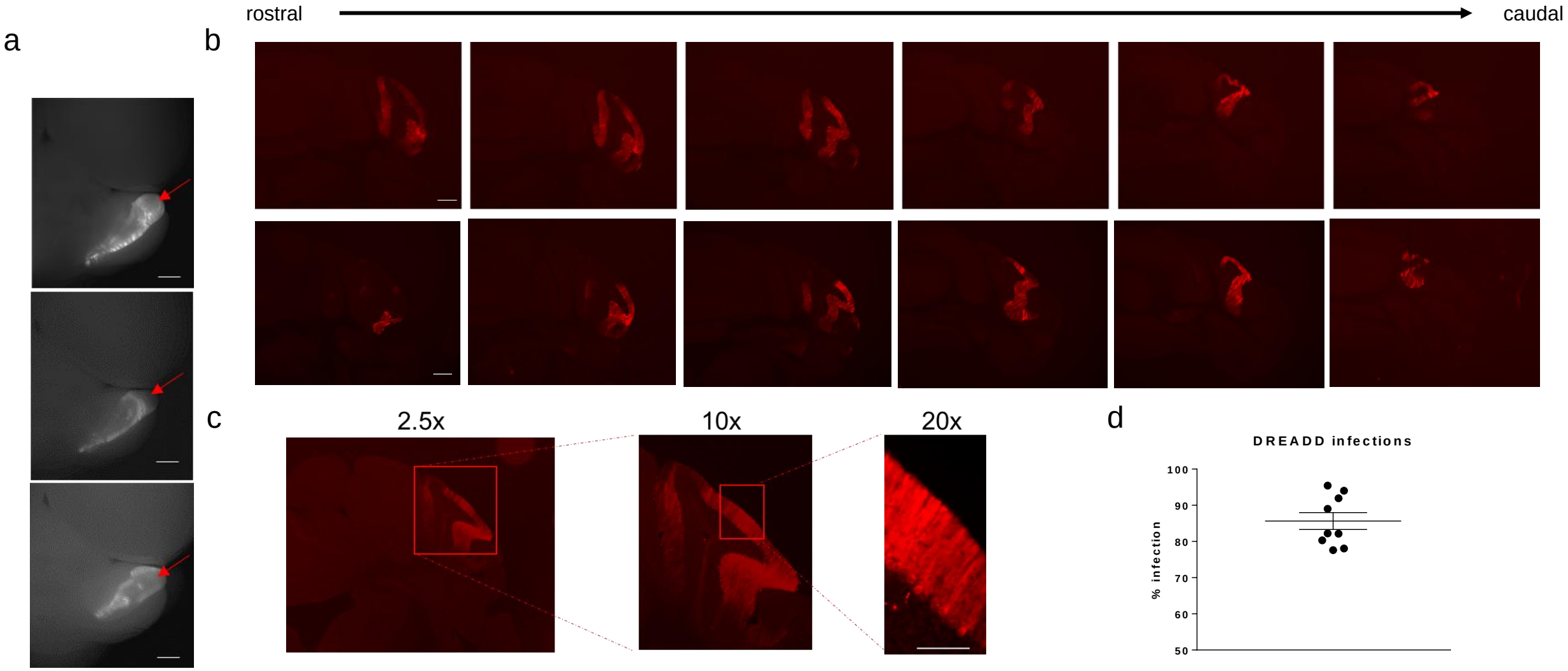

Supplementary Figure S2. DREADD expression restricted to cerebellar PNs in RCrusI. a, b. Infection of L7^{Cre} mice with AAV DREADD viruses marked by *mcherry* expression. a. Low power stereomicroscope imaging showing targeting of RCrusI (red arrows) in three different mice. Scale bars 1mm. b. Representative coronal sections from two animals through cerebellum showing DREADD (red) in RCrusI, rostral (left) to caudal (right) Scale bar 200 μm. c. Representative coronal sections through RCrusI (highlighted by red boxes in 2.5x) showing Purkinje neuronal expression. Scale bar 100 μm. d. Total percentage of infected cells (mcherry+) compared to number of total PCs quantified by calbindin staining. Error bars represent S.E.M.

a

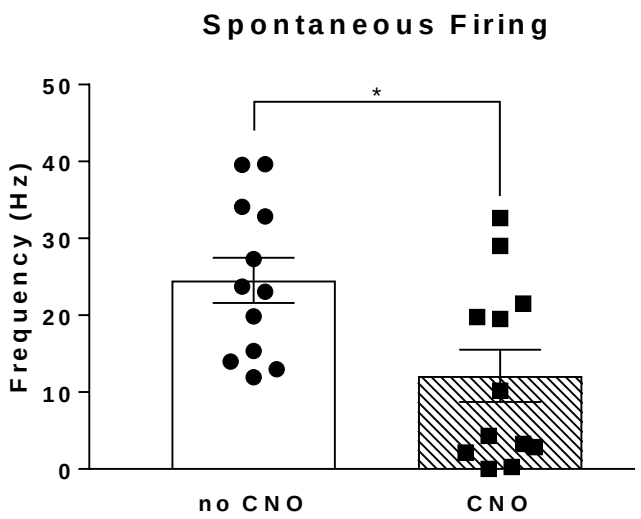

b

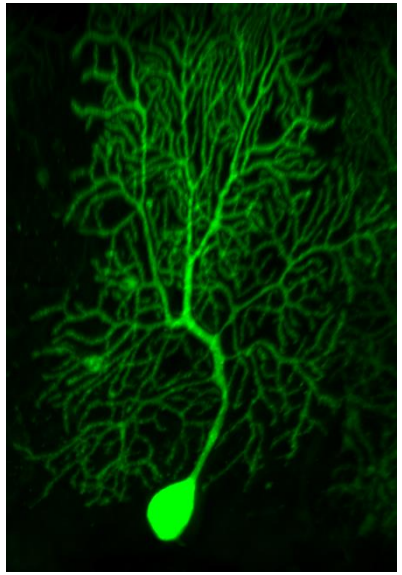

Supplementary Figure S3. Spontaneous Firing Frequency in DREADD infected Purkinje neurons. a. Acute slice recordings from PNs in RCrusI infected with hM4Di (inhibitory DREADD) showingspontaneous firing frequency with addition of CNO (n=12 cells per group, 7 animals). b. PNs were identified by characteristic morphology. Recorded cells were filled with biocytin and imaged to confirm identity as PNs. T-test, * p = 0.0115. Error bars represent S.E.M.

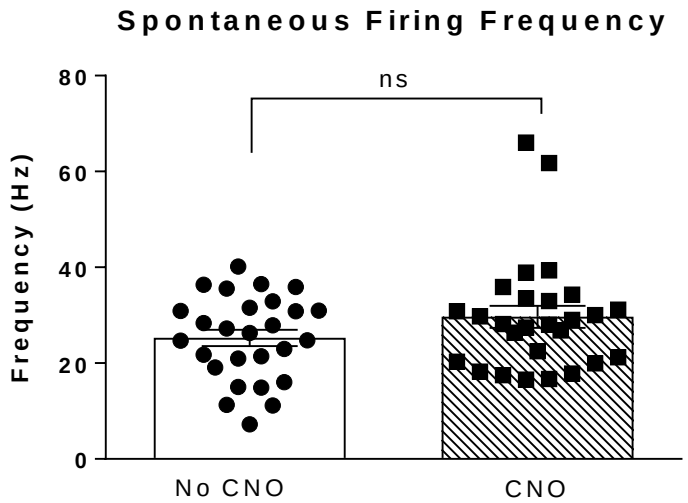

Supplementary Figure S4. Spontaneous Firing Frequency in non-infected cells in adjoining lobules to DREADD infected lobules. a. Acute slice recordings from non-infected (mcherry negative) PNs in lobules (VI, CrusI, and CrusII) adjacent to infected cells showing spontaneous firing frequency with addition of CNO (n=27 cells, 10 animals). T-test, ns, p = 0.3101. Error bars represent S.E.M.

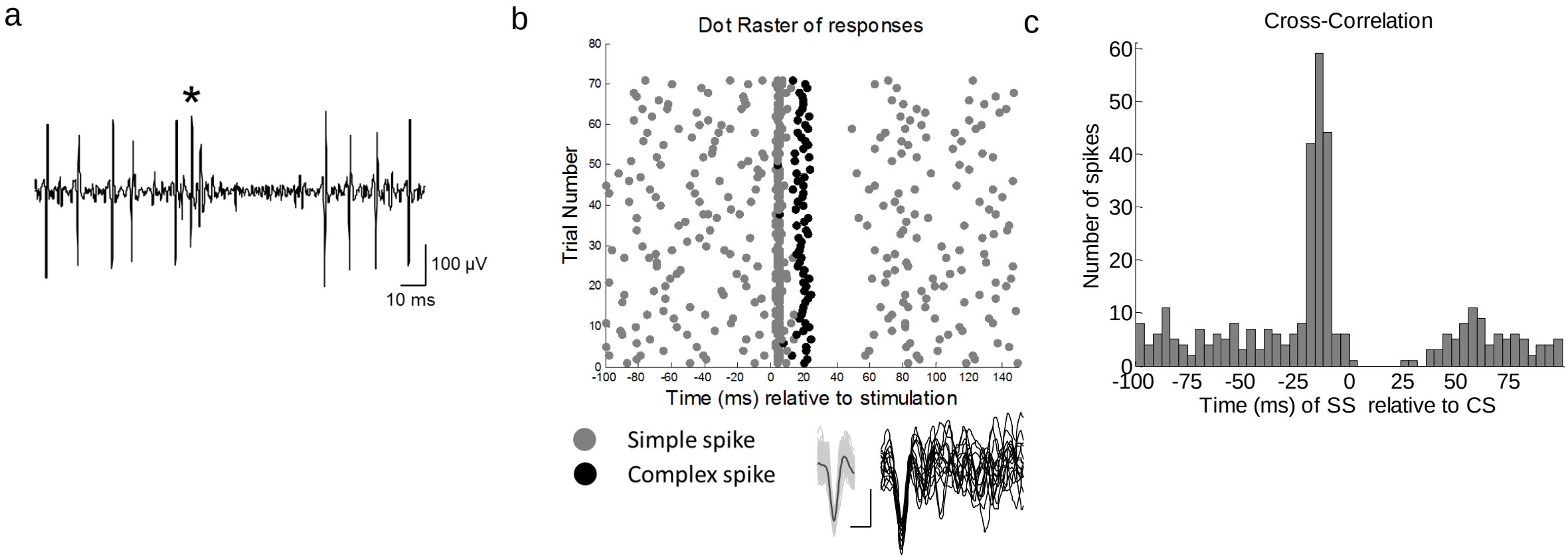

Supplementary Figure S5. Isolation of Complex Spikes from *in vivo* extracellular recordings. Complex spike isolation to confirm extracellular recordings derived from PN layer. a. Trace from spontaneous recordings (* identifies complex spike). b. Dot raster of seventy-one trials of whiskerpad evoked complex spikes in PN layer. Note impact on simple spikes with occurrence of a complex spike. Bottom: Exemplar superimposed simple and complex spike waveforms. Scalebar: 500µS/100µV. c. Cross-correlogram depicting impact of complex spike on simple spikes.

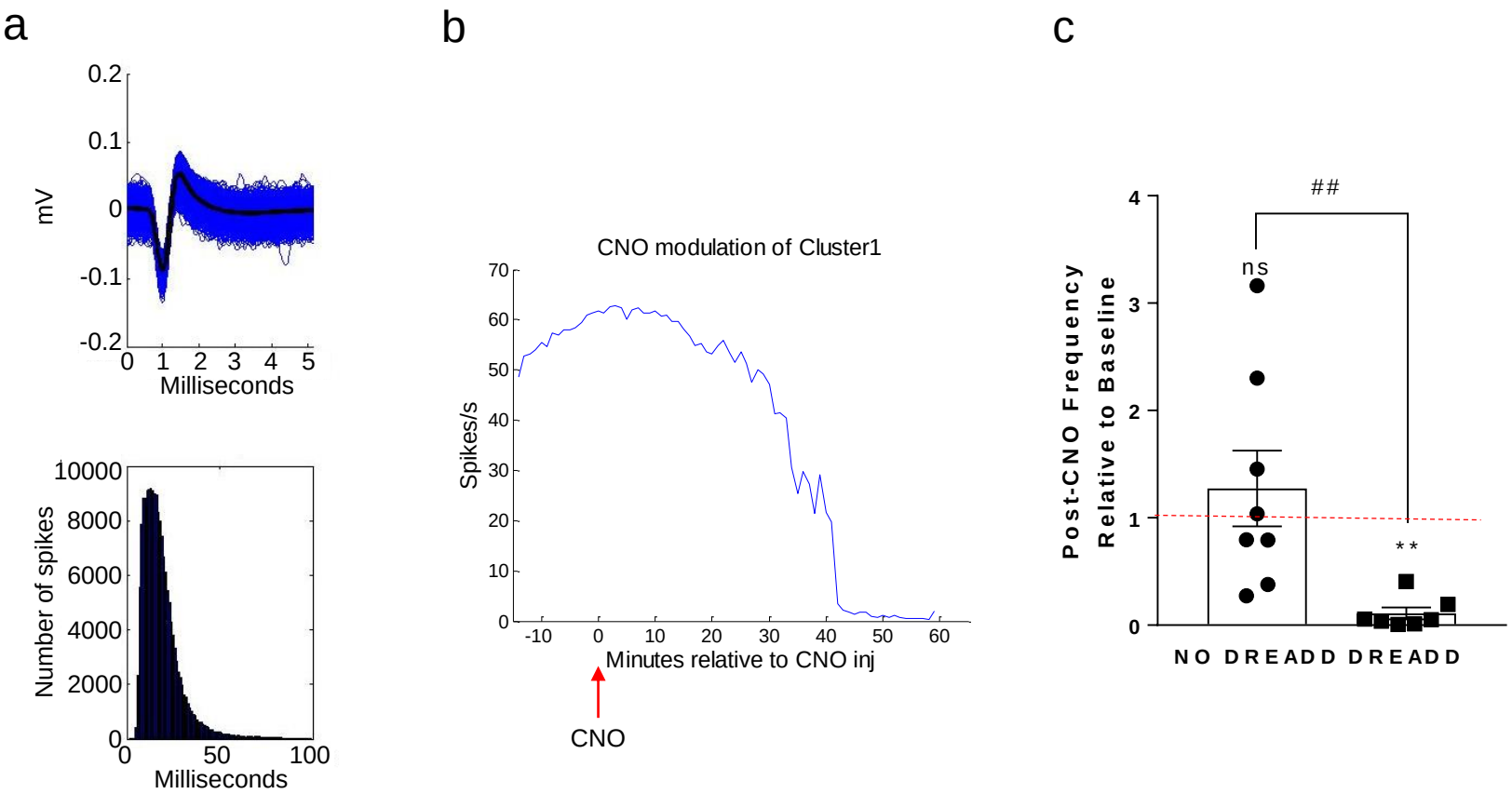

Supplementary Figure S6. *In vivo* Purkinje neuronal extracellular recordings. a. Exemplar single unit spike waveform shapes sorted using Wave_Clus (above) with the average spike waveform (black curve) superimposed on 150 spike waveforms (blue). A histogram of their interspike intervals is plotted below. b. Representative graph of CNO effect on simple spike firing rate. c. Summary of *in vivo* PN response to CNO in mock infected (No DREADD, left) and infected (DREADD, right) animals at 60 minutes (n=8 [no DREADD], n=7 [DREADD]). Baseline (dashed red line) vs. 1 hour CNO (Ratio paired t-test) ns, p=0.8922; ** p=0.0020; t-test: ##, p=0.0232. Error bars represent S.E.M.

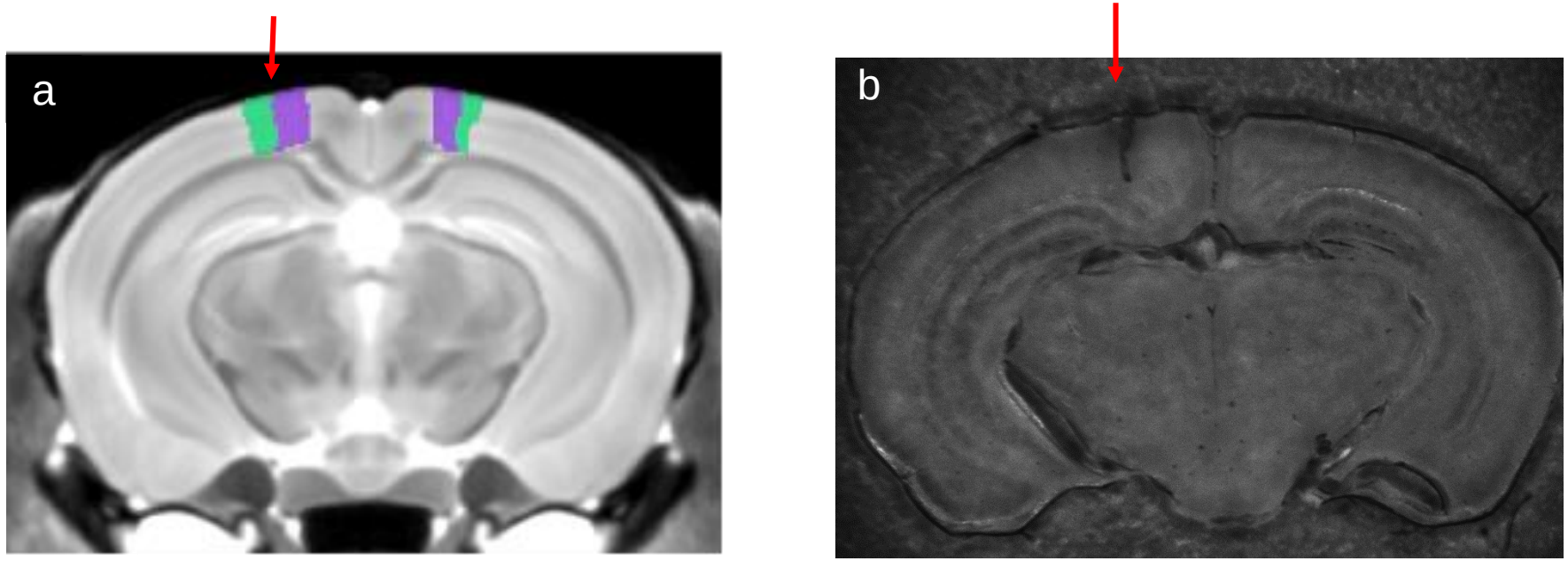

Supplementary Figure S7. Site of *in vivo* parietal single unit recordings. a. Schematic modified from Ullman et al., 2014 showing medial (purple) and lateral (green) parietal association areas. b. Location of electrode placement (marked by red arrows). Cortical mark generated with bipolar stimulation electrode.

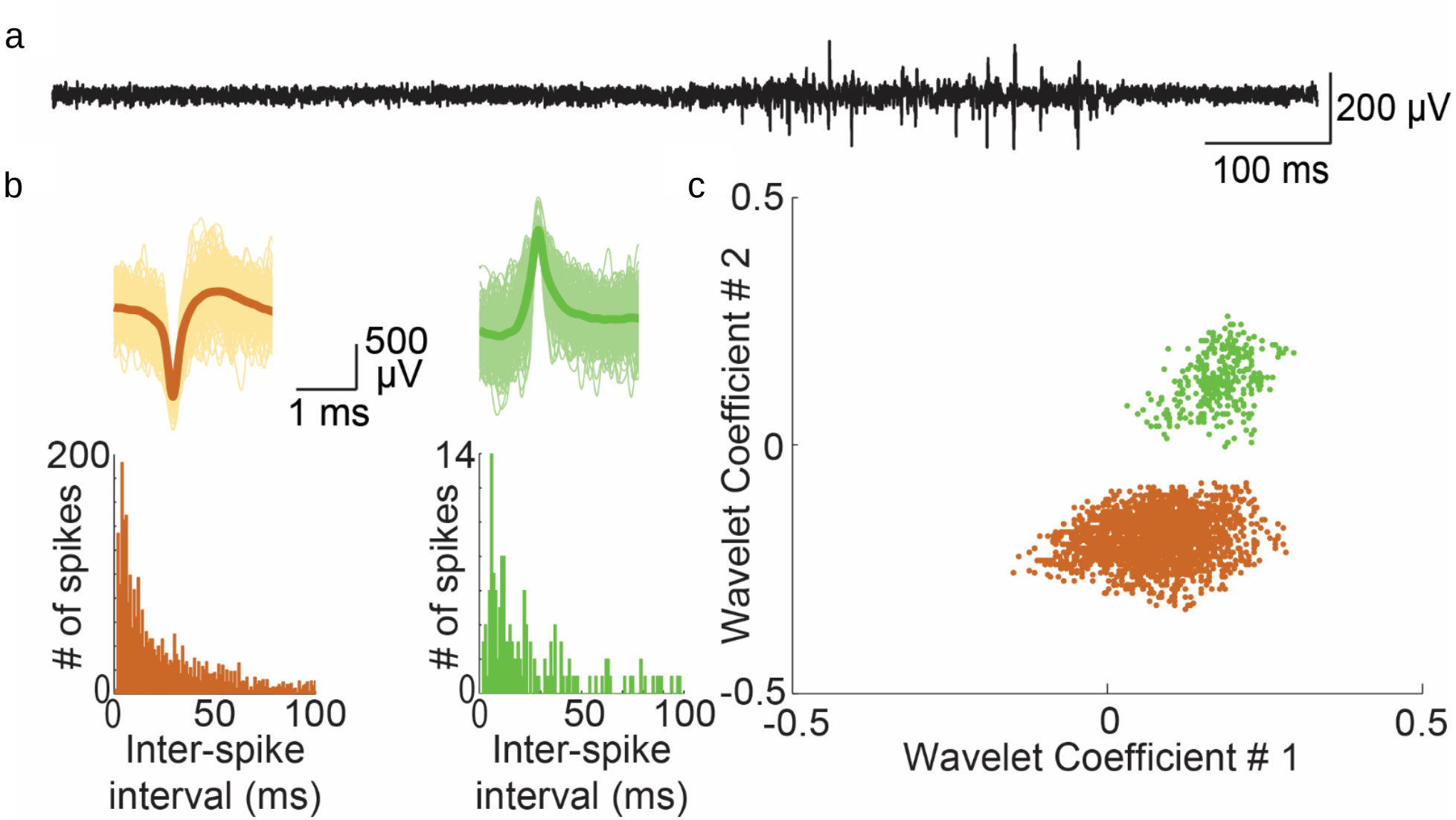

Supplementary Figure S8. Single unit spike sorting. a. One second continuous band-pass-filtered extracellular recording from the left parietal association cortex of mice with spontaneous multiunit spikes. b. Exemplar single unit spike waveform shapes sorted using Wave_Clus (top) with a histogram of their interspike intervals plotted below. The average spike waveform (dark color) is superimposed on 150 spike waveforms (light color). c. Projection of spike shapes onto the feature space of wavelet coefficients indicates distinct clusters to allow grouping of similar shaped waveforms.

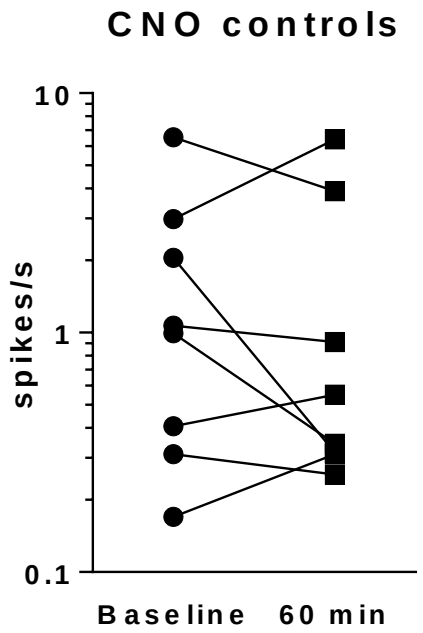

Supplementary Figure S9. No significant change in single units in parietal association areas in non-DREADD RCrusI injection. In control mice with non-DREADD RCrusI injection, single unit spike rates in parietal association areas were recorded with CNO treatment (n=8). Ratio, paired t-test, p>0.9999.

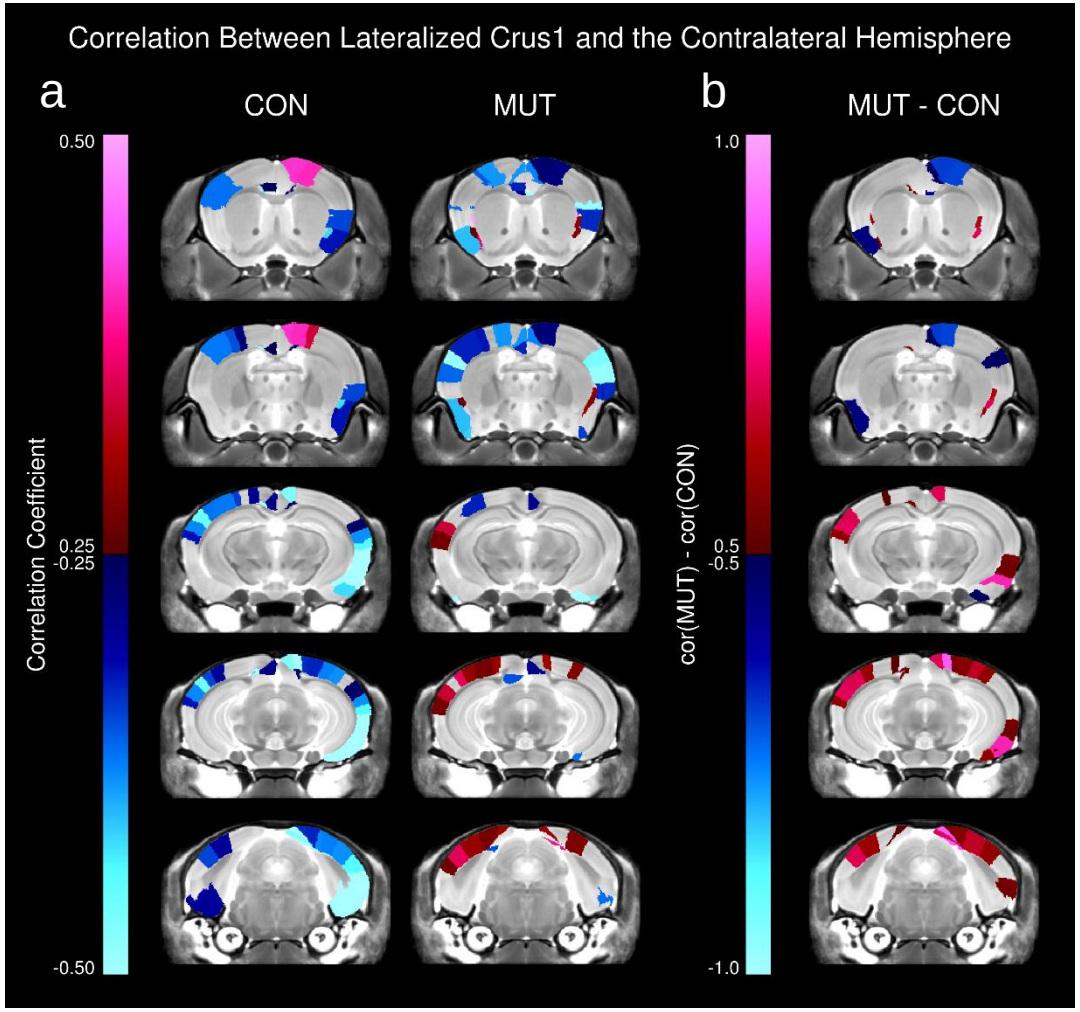

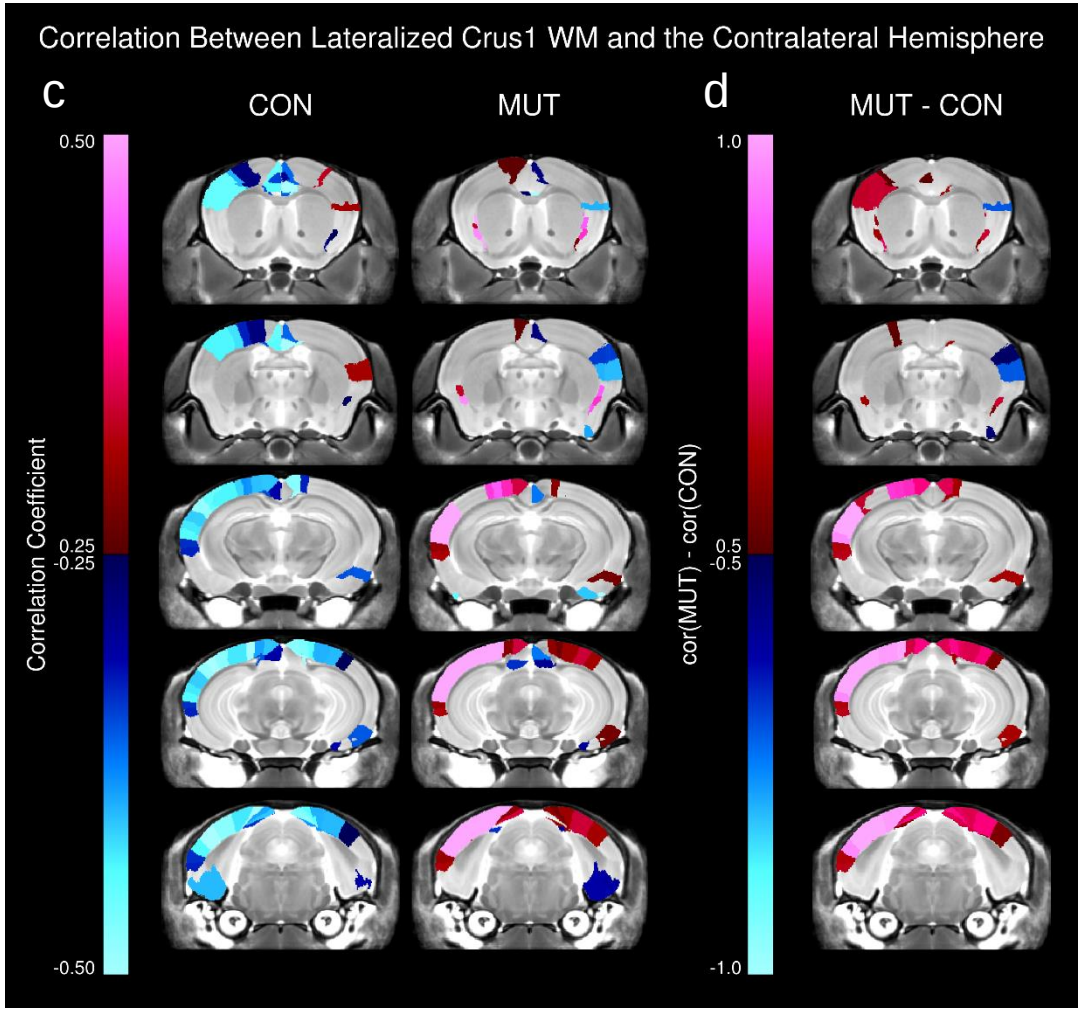

Supplementary Figure S10. Structural connectivity MRI reveals differentially lateralized connectivity between CrusI (left) or CrusI white matter (WM) (right) and contralateral hemisphere. Heatmap of connectivity superimposed on MRI-derived brain regions illustrates connectivity with contralateral CrusI. Examination of connectivity by structural covariance MRI (scMRI) examines a., c. lateralization of structural connectivity between contralateral hemispheres and RCrusI and LCrusI in control (CON) and mutant (MUT) animals. b., d. Differences in connectivity between CON and MUT cohorts summarized.

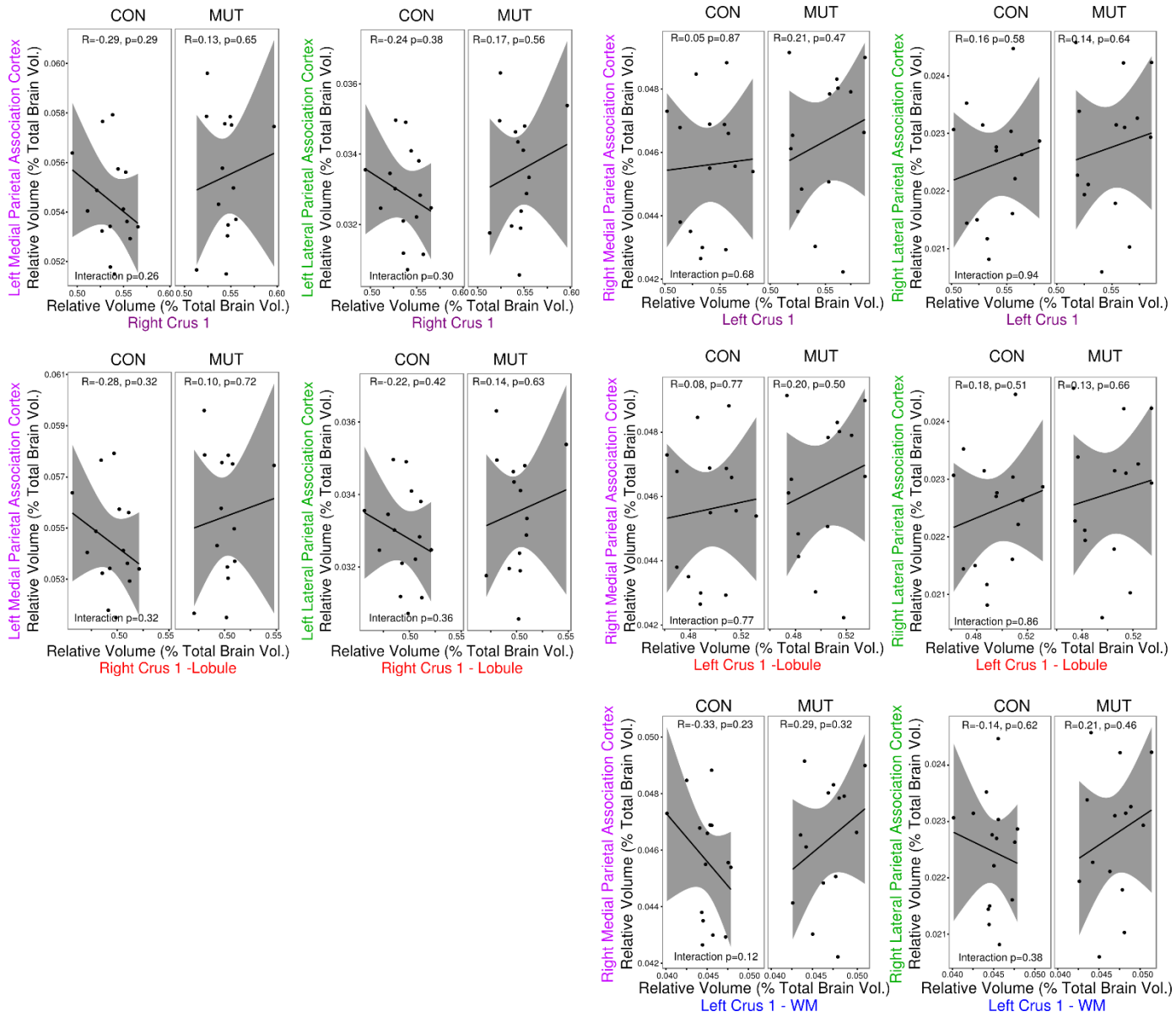

Supplementary Figure S11. Structural connectivity MRI examining connectivity between RCrusI and parietal cortical association areas in control and mutant mice.

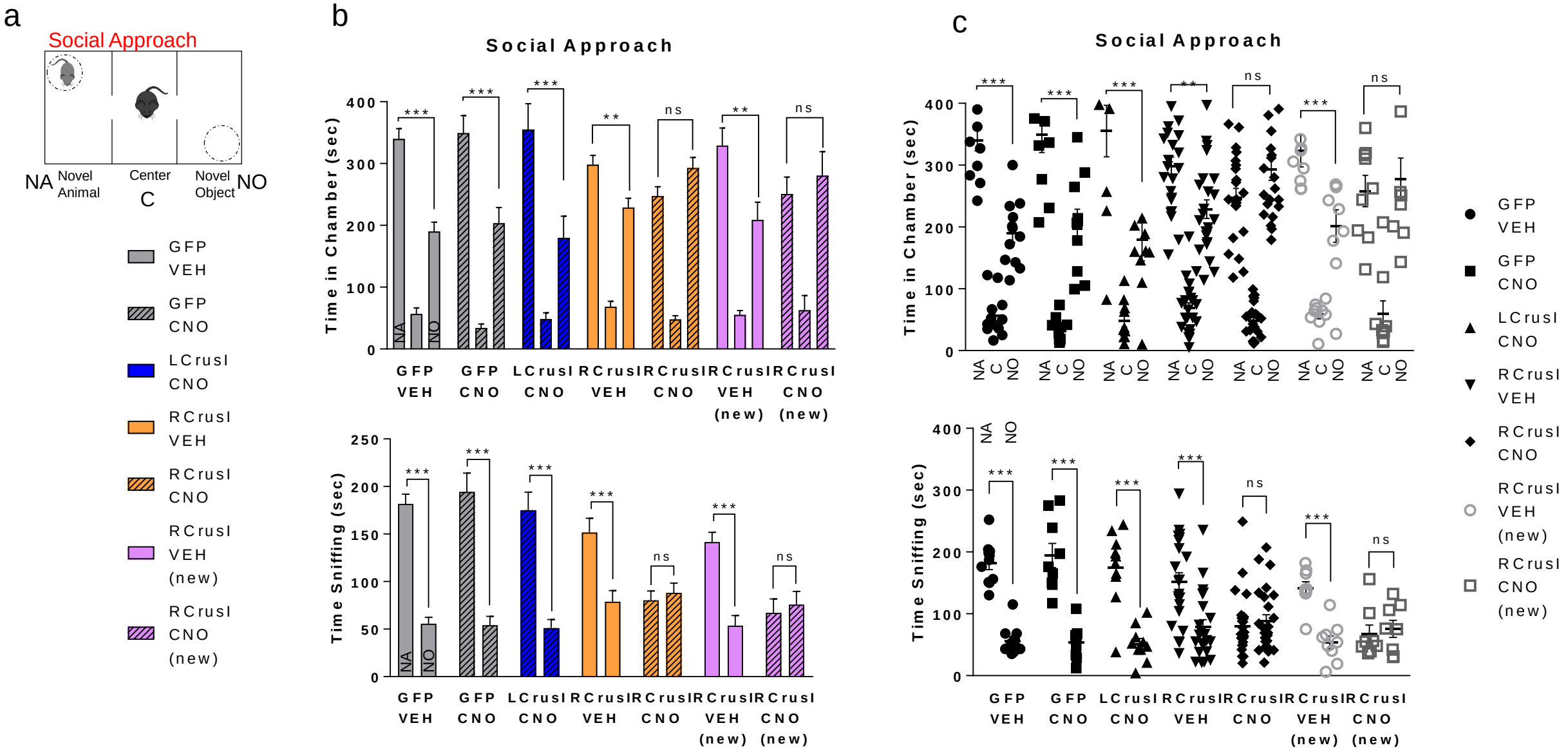

Supplementary Figure S12. Chemogenetic-mediated inhibition of RCrusI results in impaired social approach. a. Schematic of three-chambered apparatus and social approach paradigm. b, c. Social approach testing in three-chambered apparatus shown with Time in Chamber (top) and Time sniffing (bottom). Cohorts include: GFP injected into RCrusI, hMD4i injected into LCrusI, and hMD4i injected into RCrusI upon treatment with vehicle (VEH) or clozapine-N-oxide (CNO). Additional cohort (new) performed to further examine effects of chemogenetic-mediated RCrusI inhibition. For clarity, data is separated into summary bar graphs (b) and individual data points (c). Two-way ANOVA, Bonferroni post-hoc analysis. *** p<0.001; ** p<0.01; ns=not significant. Error bars represent S.E.M. NA=novel animal; C=center; NO=novel object.

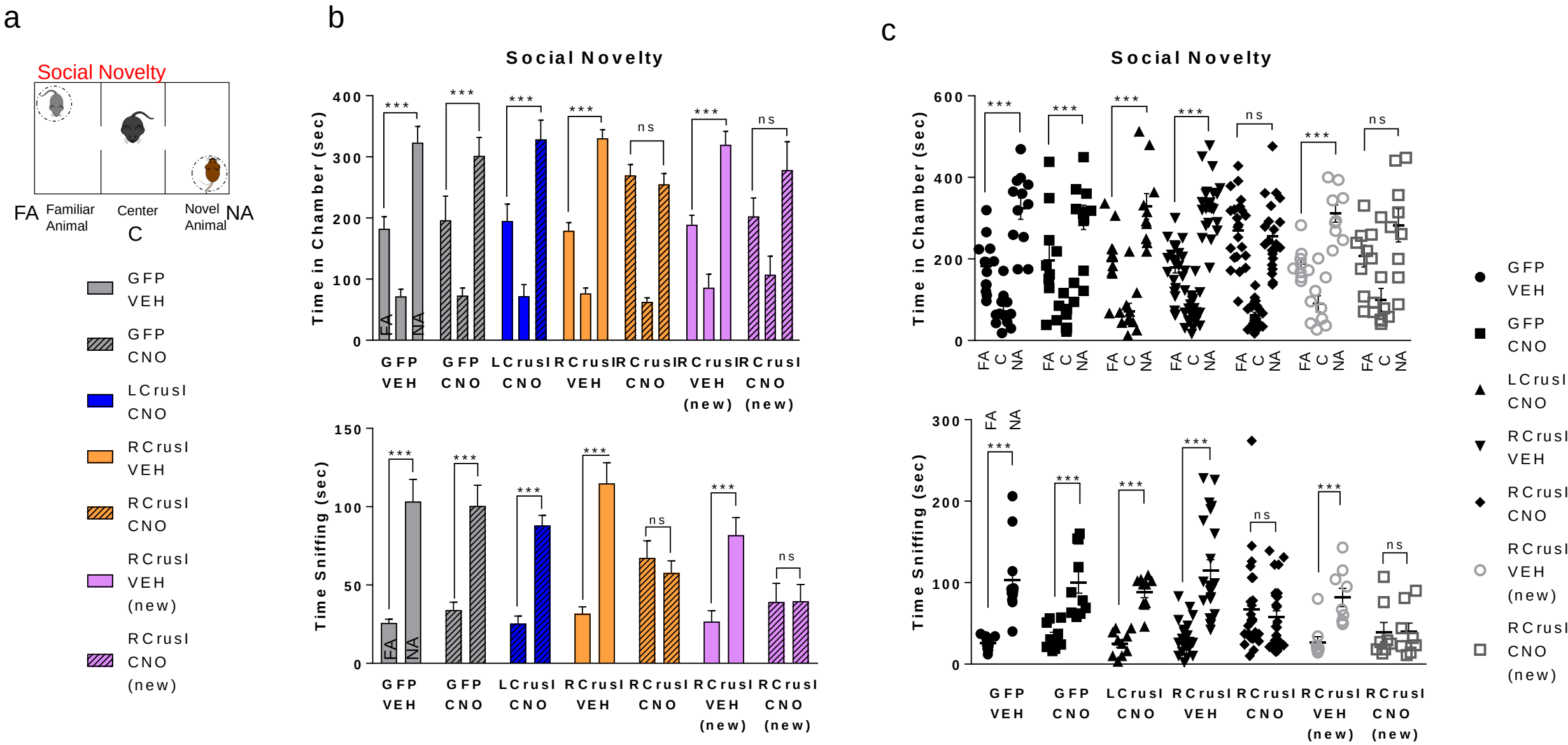

Supplementary Figure S13. Chemogenetic-mediated inhibition of RCrusI results in impaired social novelty. a. Schematic of social novelty paradigm. b. Social novelty testing in three-chambered apparatus shown with Time in Chamber (top) and Time sniffing (bottom). Cohorts include: GFP injected into RCrusI, hMD4i injected into LCrusI, and hMD4i injected into RCrusI upon treatment with vehicle (VEH) or clozapine-N-oxide (CNO). Additional cohort (new) performed to further examine effects of chemogenetic-mediated RCrusI inhibition. For clarity, data is separated into summary bar graphs (b) and individual data points (c). Two-way ANOVA, Bonferroni post-hoc analysis. *** $p<0.001$; ** $p<0.01$; Error bars represent S.E.M. ns=not significant. NA=novel animal; C=center; FA=familiar animal.

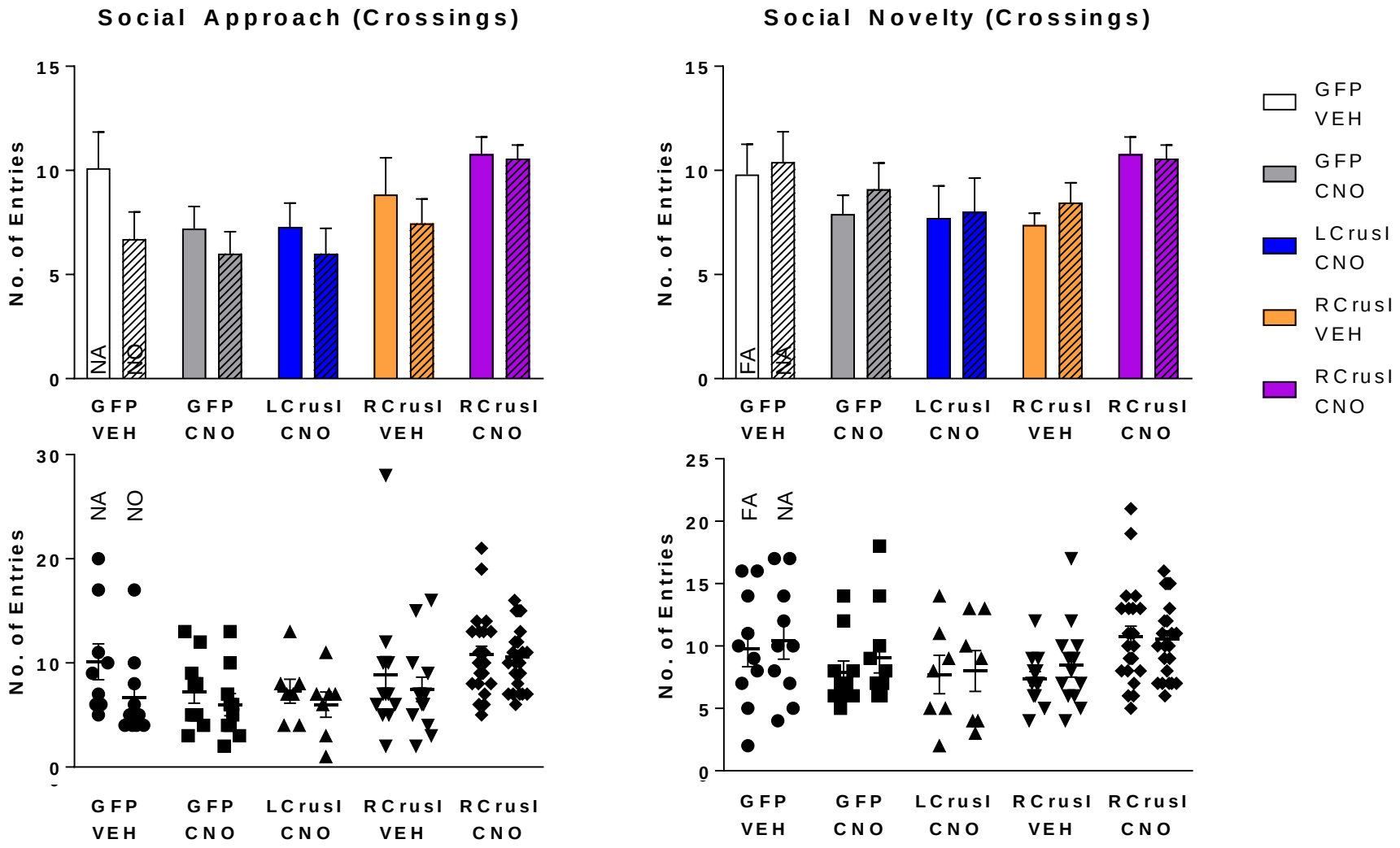

Supplementary Figure S14. Locomotor activity in the three-chambered apparatus is comparable between all groups regardless of genotype or chemogenetic-mediated inhibition. Social approach (left; number of entries into chamber with novel animal vs. novel object (hatched bars)) and Social Novelty (right; number of entries into chamber with familiar animal vs. novel animal (hatched bars)). Summary group data (above) and individual data points (below). Two-way ANOVA, Bonferroni post-hoc analysis. All comparisons are not significant, ns, $p>0.05$. Error bars represent S.E.M. NA=novel animal; NO=novel object; FA=familiar animal.

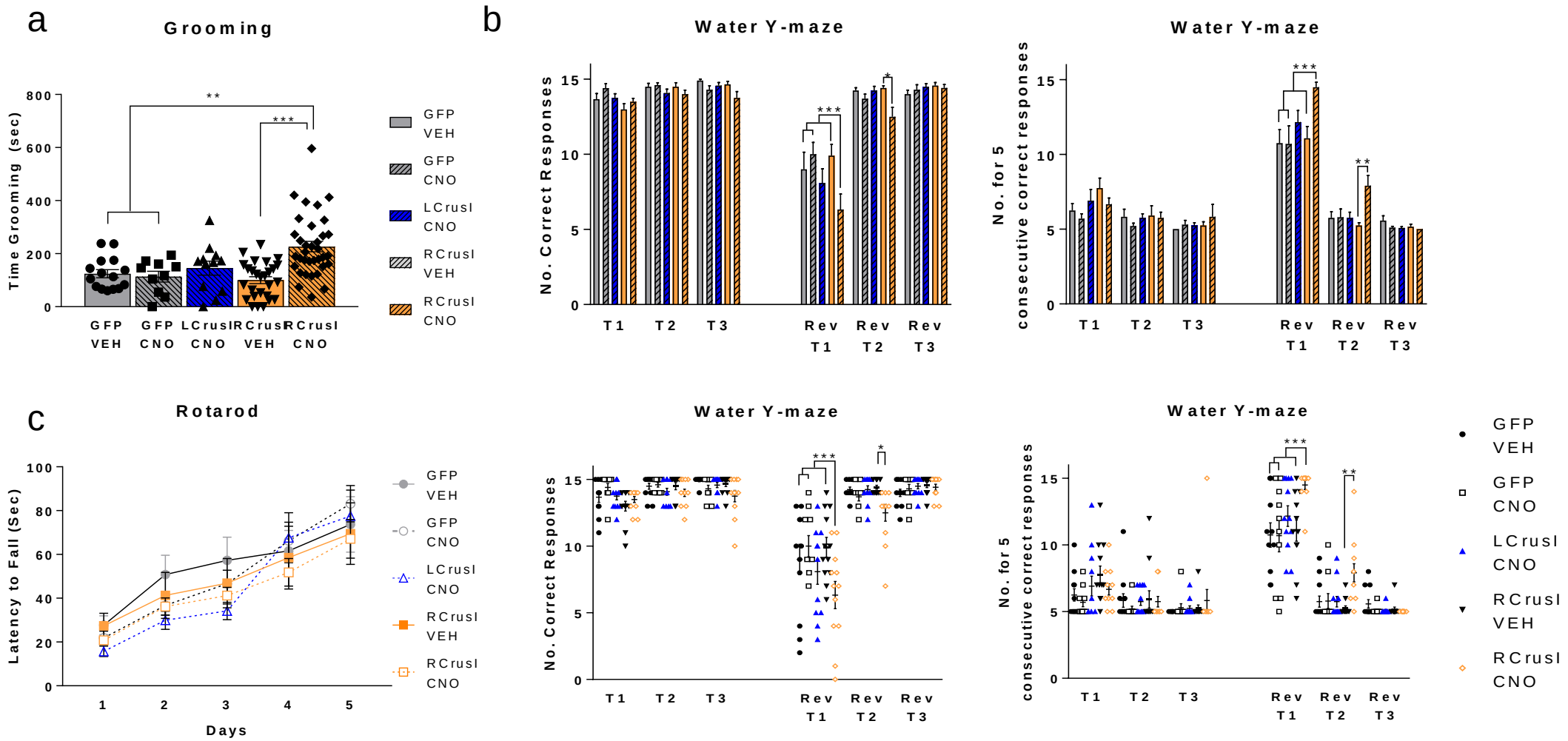

Supplementary Figure S15. Chemogenetic-mediated inhibition of RCrusI results in repetitive and inflexible behaviors. Cohorts examined include: GFP injected into RCrusI, hMD4i injected into LCrusI, and hMD4i injected into RCrusI upon treatment with vehicle (VEH) and clozapine-N-oxide (CNO). a. Repetitive grooming, b. water Y-maze (number of correct responses (left) and number of trials needed to generate 5 correct responses (right)) were examined. Individual data points are plotted below for clarity. c. Rotarod was also examined without significant changes across conditions. Two- or one-way ANOVA, Bonferroni post hoc analysis. *** $p<0.001$; ** $p<0.01$; * $p<0.05$; ns=not significant. Error bars represent S.E.M.

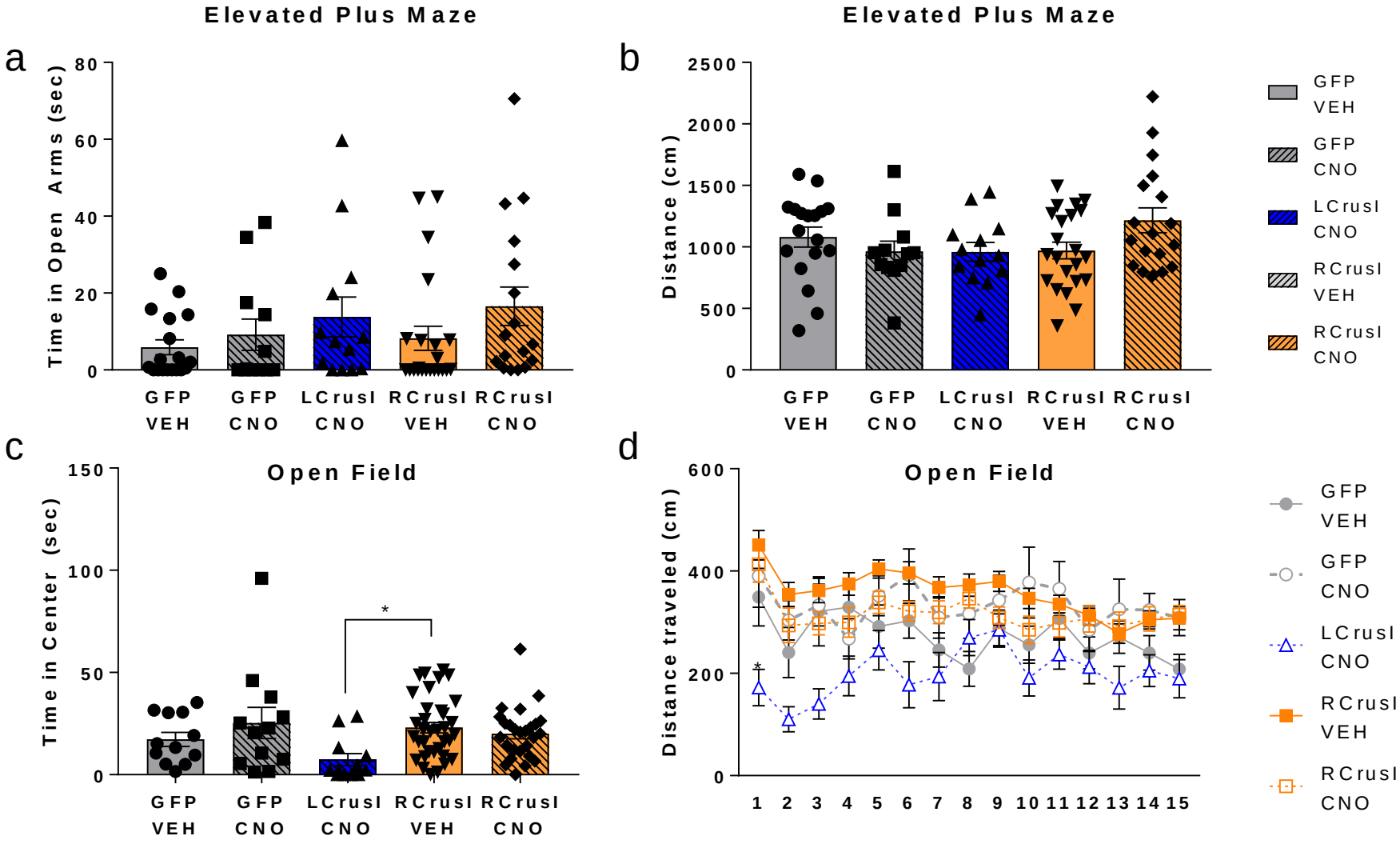

Supplementary Figure S16. Chemogenetic-mediated inhibition of RCrusI does not alter anxiety or locomotor behaviors. Elevated plus maze a. (time in open arms) and b. (distance traveled) and open field c. (time in center) and d. (distance traveled) were examined. Two- or one-way ANOVA, Bonferroni post hoc analysis. * $p<0.05$; all other comparisons are not significant. Error bars represent S.E.M.

a

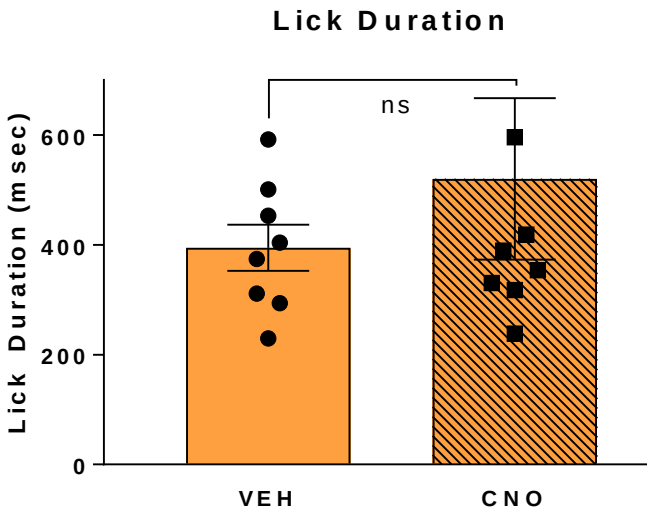

b

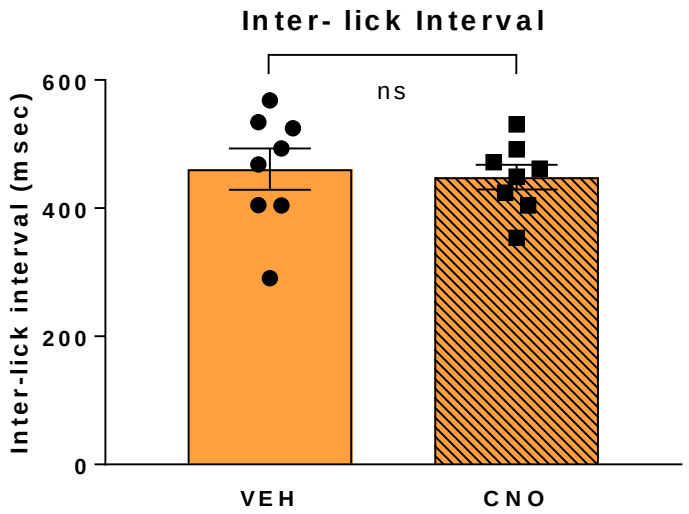

Supplementary Figure S17. Rhythmic licking. Rhythmic licking was examined with chemogenetic-mediated inhibition (CNO) of RCrusI; a. lick duration (ns, p=0.4265) and b. inter-lick interval (ns, p=0.7404). T-test. Error bars represent S.E.M.

a

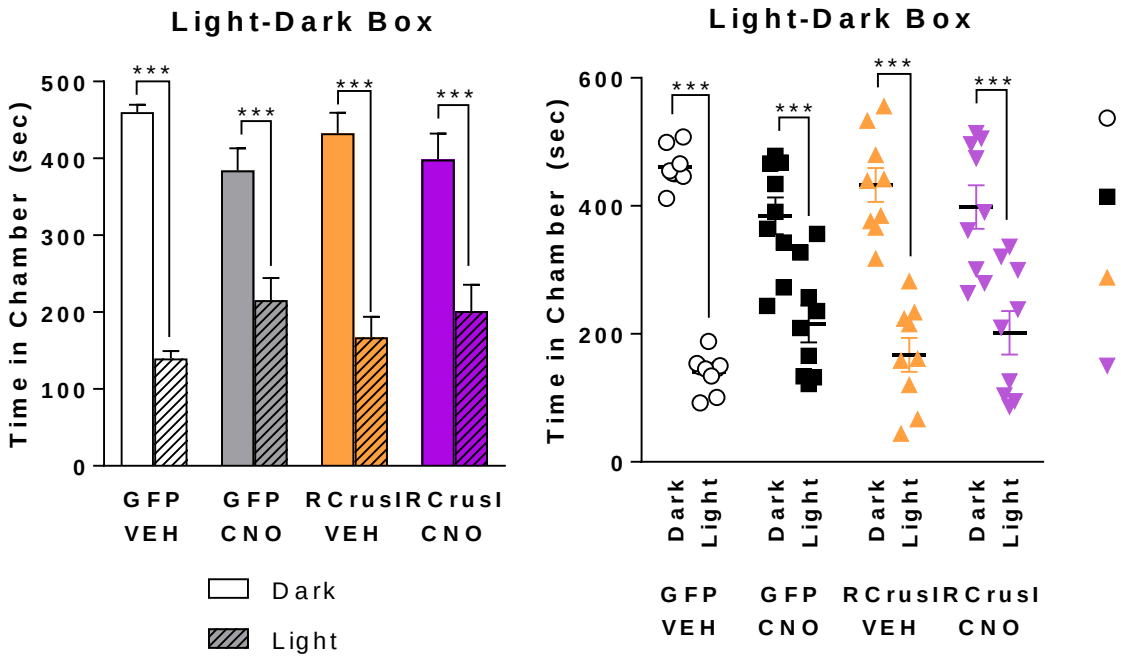

b

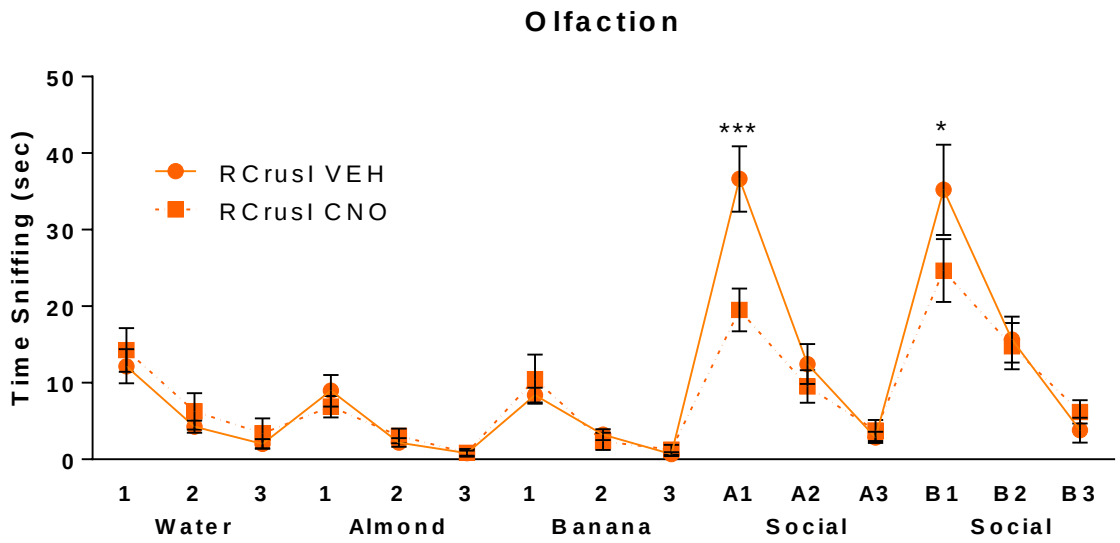

Supplementary Figure S18. Anxiety and sensory behaviors. a. Light-Dark box testing. Summary graph on left, individual data points on right. b. Olfactory testing using dishabituation-habituation olfactory testing paradigm. Two- or one-way ANOVA, Bonferroni post hoc analysis. *** $p<0.001$, * $p=0.0206$. Error bars represent S.E.M.

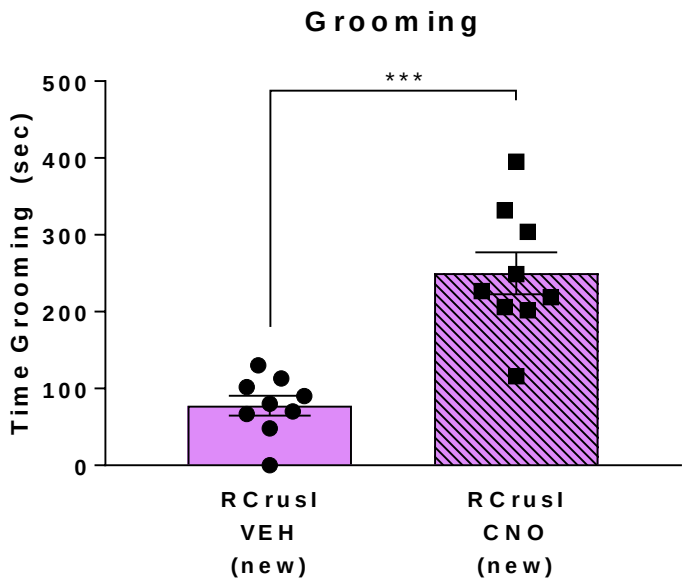

Supplementary Figure S19. Grooming. DREADD mediated inhibition of RCrusI in an independent (new) cohort, n=9 (VEH) / 10 (CNO)**.** T-test. *** p=0.0009. Error bars represent S.E.M.

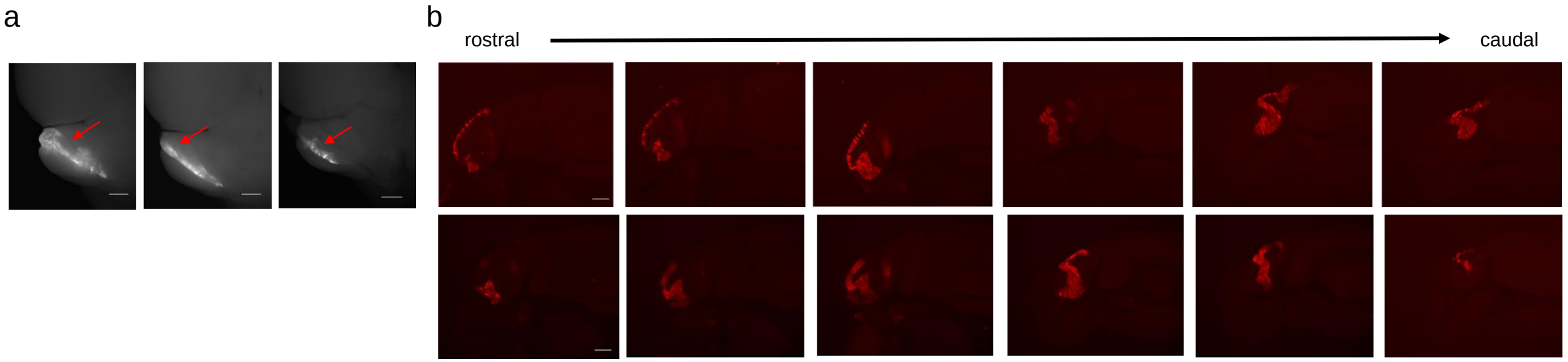

Supplementary Figure S20. DREADD expression restricted to LCrusI. a, b. Infection of L7^{Cre} mice with AAV DREADD viruses show infection of PNs marked by *mcherry* expression. a. Low power stereomicroscope imaging showing targeting of LCrusI (red arrows) in three different mice. Scale bars 1mm. b. Representative coronal sections through cerebellum from two animals showing targeting of DREADD (red) to LCrusI, rostral (left) to caudal (right). Scale bar 200 μm.

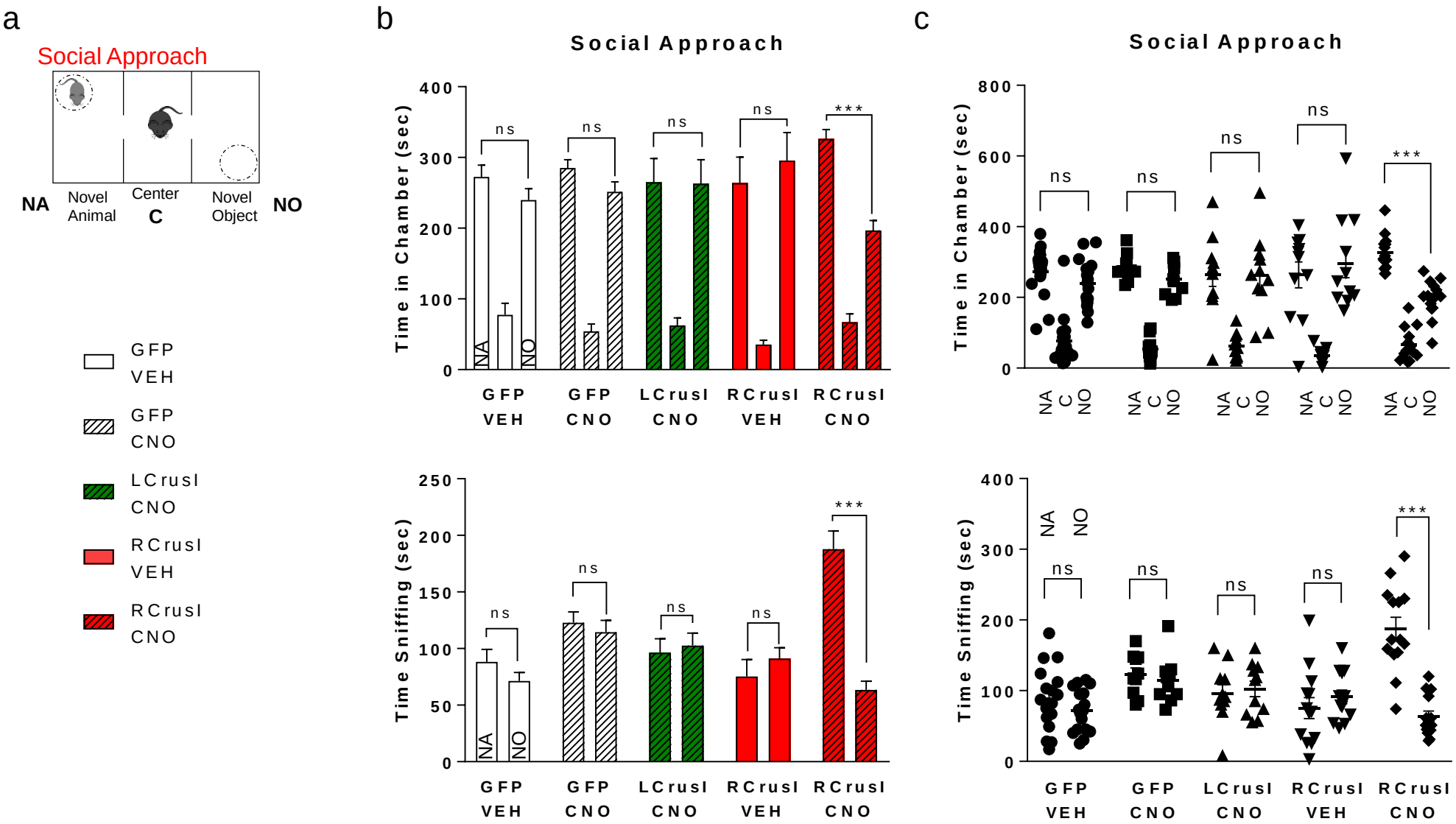

Supplementary Figure S21. Chemogenetic activation of RCrusI rescues social approach behavior in PN *Tsc1* mutant mice. a. Schematic of three-chambered apparatus, social approach paradigm. b., c. CNO-mediated PN stimulation in mutant mice. b. summary plot and c. individual data points graphed separately for clarity. Two-way ANOVA, Bonferroni post hoc analysis. *** p<0.001; ns=not significant. Error bars represent S.E.M. NA=novel animal; C=center; NO=novel object.

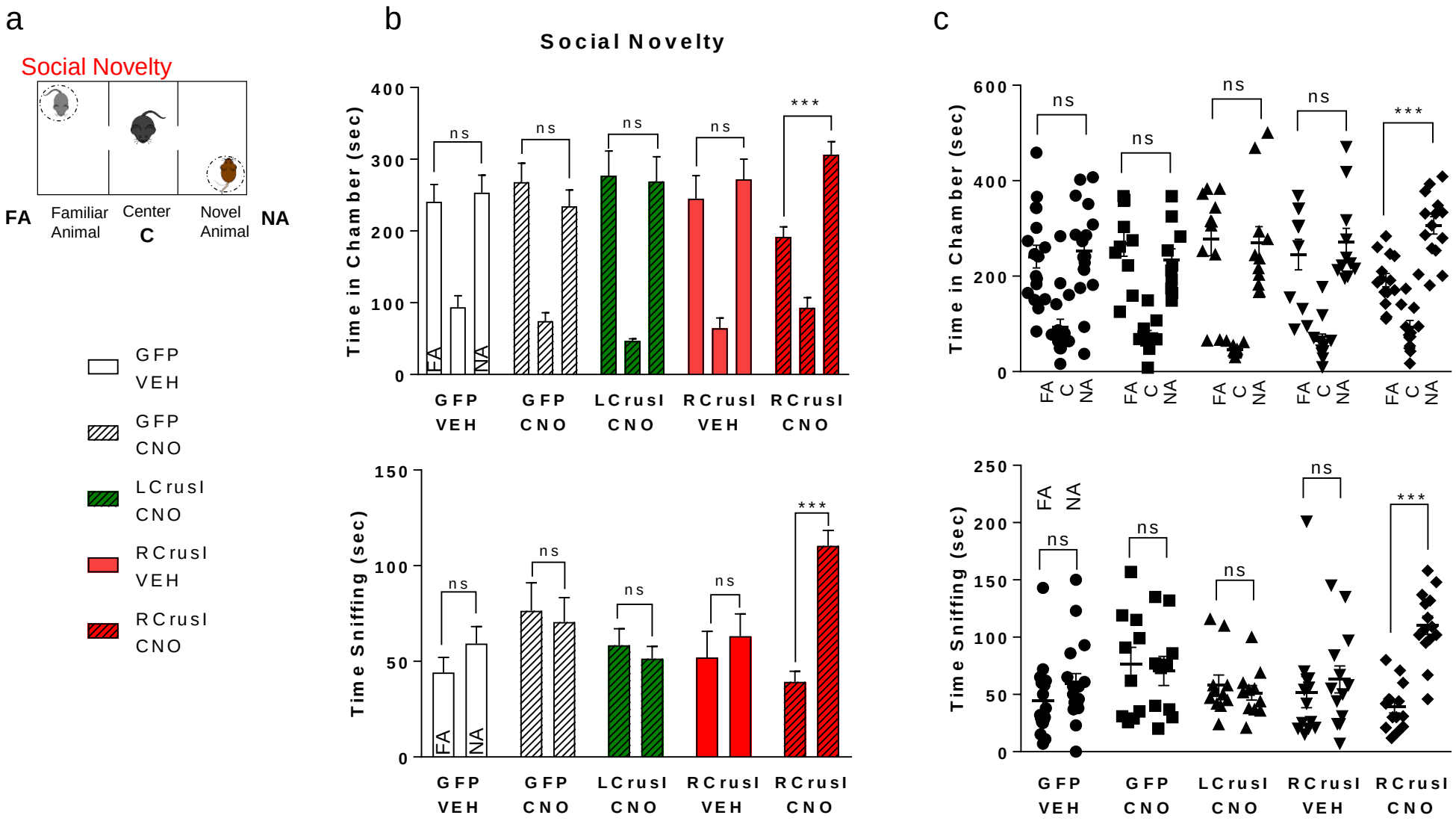

Supplementary Figure S22. Chemogenetic activation of RCrusI rescues social novelty behavior in PN *Tsc1* mutant mice. a. Schematic of three-chambered apparatus, social novelty paradigm. b., c. CNO-mediated PN stimulation in mutant mice. b. summary plot and c. individual data points graphed separately for clarity. Two-way ANOVA, Bonferroni post hoc analysis. *** p<0.001; ns=not significant. Error bars represent S.E.M. NA=novel animal; FA=familiar animal.

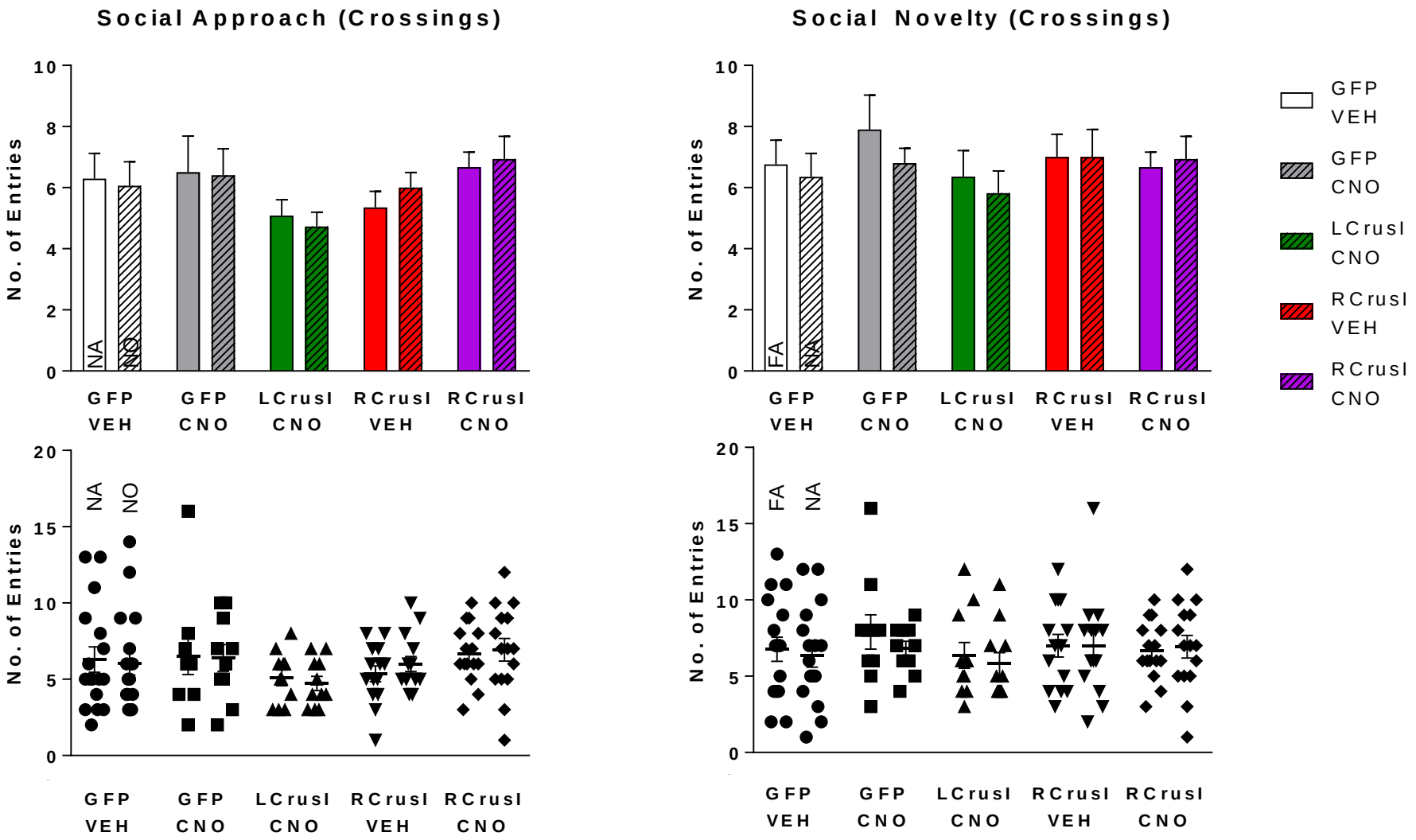

Supplementary Figure S23. Locomotor activity in the three-chambered apparatus is comparable between all groups regardless of genotype or chemogenetic-mediated stimulation. Social approach (left; number of entries into chamber with novel animal vs. novel object (hatched bars)) and Social Novelty (right; number of entries into chamber with familiar animal vs. novel animal (hatched bars)). Summary group data (above) and individual data points (below). Two-way ANOVA, Bonferroni post hoc analysis. No significant differences are seen between all groups, $p>0.05$. Error bars represent S.E.M. NA=novel animal; NO=novel object; FA=familiar animal.

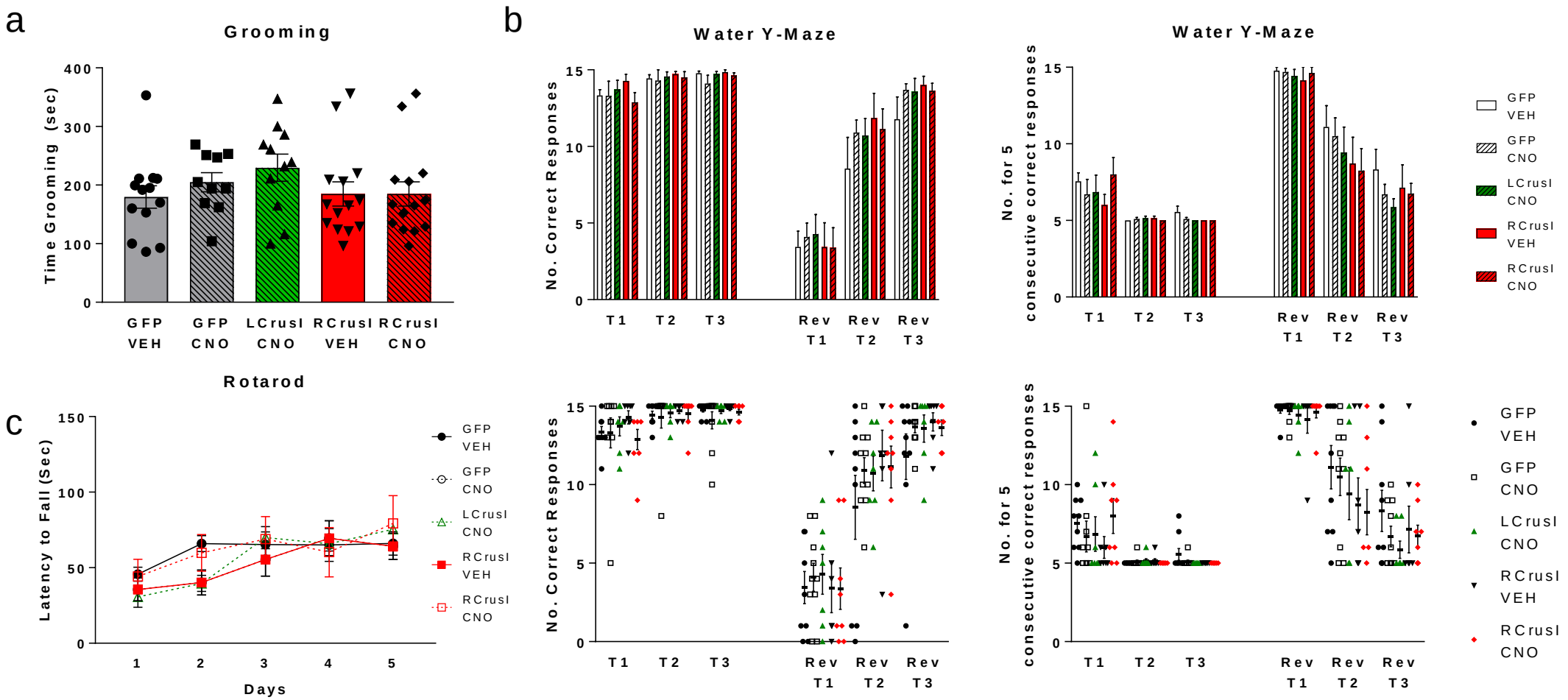

Supplementary Figure S24. Chemogenetic-mediated stimulation of RCrusI in PN *Tsc1* mutant mice does not rescue repetitive or inflexible behaviors. a. Repetitive grooming, b. reversal learning impairment in Water Y-Maze (summary data above and individual data points plotted below for clarity), and c. rotarod with chemogenetic-mediated stimulation of RCrusI. Two-way or one-way ANOVA, Bonferroni post hoc analysis. All data show no significant differences between groups. Error bars represent S.E.M.

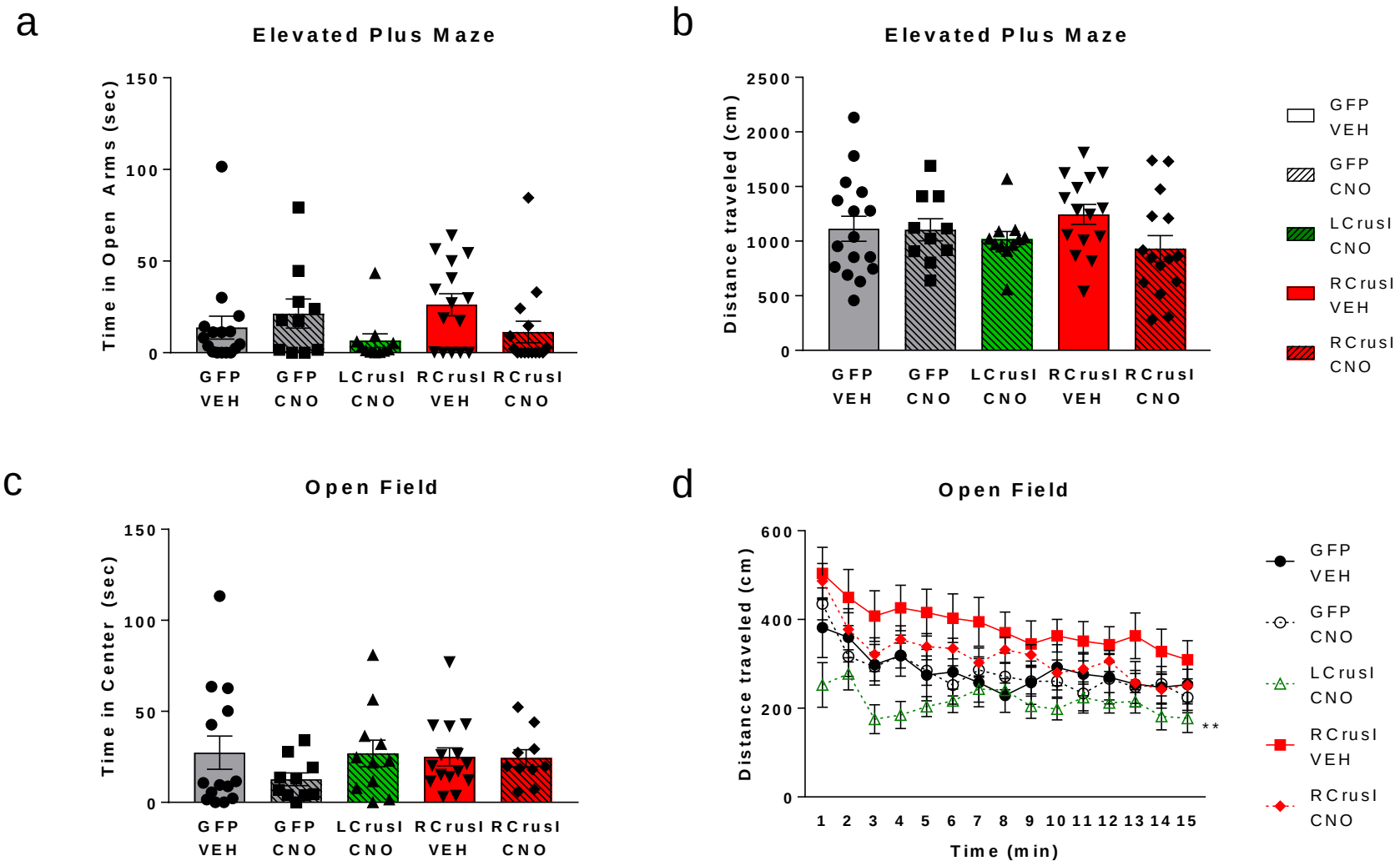

Supplementary Figure S25. Chemogenetic-mediated stimulation of RCrusI in PN *Tsc1* mutant mice does not impact locomotor or anxiety-related behaviors. a. Open arm exploration and b. distance traveled in the elevated plus maze with CNO-mediated stimulation of RCrusI in PN *Tsc1* mutant mice. In open field testing, c. time in center and d. distance traveled were examined. Two-way or one-way ANOVA, Bonferroni post hoc analysis. ** p=0.0019. All others show no significant differences between groups. Error bars represent S.E.M.

Supplementary Information

Supplementary Tables

Supplementary Table 1. Pre-tDCS functional connectivity from RCrusI seeds

Seed	Location	Clusters (x,y,z)	size	cluster p-FWE	cluster p-FDR	cluster p-unc	peak p-FWE	peak p-unc
Right Crus I Correlations	Right Crus I	(+46 -64 -34)	28726	<0.0001	<0.0001	<0.0001	<0.0001	<0.0001
	Left medial superior frontal gyrus	(-08 +38 +52)	19324	<0.0001	<0.0001	<0.0001	<0.0001	<0.0001
	Left angular gyrus	(-46 -52 +34)	3787	<0.0001	<0.0001	<0.0001	0.0001	<0.0001
	Right inferior temporal gyrus	(+50 -10 -36)	2212	<0.0001	<0.0001	<0.0001	0.0019	<0.0001
	Left thalamus	(-06 -04 +08)	1681	<0.0001	<0.0001	<0.0001	0.0000	<0.0001
	Left middle cingulate cortex	(-06 -44 +36)	1111	<0.0001	<0.0001	<0.0001	0.0092	<0.0001
	Right angular gyrus	(+52 -72 +42)	814	<0.0001	<0.0001	<0.0001	0.0775	<0.0001
	Right inferior frontal gyrus	(+48 +36 -20)	629	<0.0001	<0.0001	<0.0001	0.0011	<0.0001
	Left hippocampus	(-12 -14 -18)	435	0.0004	0.0001	<0.0001	0.0189	<0.0001
	Right middle frontal gyrus	(+50 +20 +50)	384	0.0009	0.0002	<0.0001	0.0512	<0.0001
Right Crus I Anti-Correlations	Right Insula	(+38 -02 +08)	4880	<0.0001	<0.0001	<0.0001	0.0002	<0.0001
	Left postcentral gyrus/precentral gyrus	(-62 -04 +30)	3955	<0.0001	<0.0001	<0.0001	0.0001	<0.0001
	Left middle cingulate cortex	(-16 -32 +46)	1244	<0.0001	<0.0001	<0.0001	0.0006	<0.0001
	Right parahippocampal gyrus	(+18 +04 -36)	436	0.0004	0.0002	<0.0001	0.0135	<0.0001
	Right superior parietal lobule/precuneus	(+16 -46 +58)	374	0.0010	0.0005	0.0001	0.0891	<0.0001
	Right superior parietal lobule/precuneus	(+16 -64 +52)	222	0.0179	0.0072	0.0010	0.5928	<0.0001
	Right postcentral gyurs	(+34 -38 +74)	169	0.0554	0.0195	0.0032	0.5558	<0.0001
DMN seed of R Crus Correlations	Left superior frontal gyrus/medial frontal cortex/anterior cingulate cortex	(-14 +38 +46)	14259	<0.0001	<0.0001	<0.0001	0.0001	<0.0001
	Right Crus I	(+28 -78 -32)	11334	<0.0001	<0.0001	<0.0001	0.0001	<0.0001
	Left middle temporal gyrus/supramarginal gyrus/angular gyrus	(-60 -32 -08)	9683	<0.0001	<0.0001	<0.0001	0.0001	<0.0001
	Right inferior temporal gyrus	(+56 -12 -34)	4620	<0.0001	<0.0001	<0.0001	0.0001	<0.0001
	Left precuneus	(-04 -52 +36)	1568	<0.0001	<0.0001	<0.0001	0.0001	<0.0001
	Right superior temporal gyrus/angular gyrus	(+60 -56 +22)	1456	<0.0001	<0.0001	<0.0001	0.0001	<0.0001
	Left hippocampus	(-22 -16 -18)	352	0.0009	0.0002	<0.0001	0.3008	<0.0001
	Left occipital cortex	(-16 -108 +02)	212	0.0158	0.0027	0.0008	0.8480	<0.0001
	Left occipital cortex	(+18 -106 +08)	210	0.0165	0.0027	0.0009	0.0677	<0.0001
	Right lobule V	(+14 -58 -16)	141	0.0829	0.0126	0.0044	0.6879	<0.0001
	Right middle occipital gyrus	(+46 -88 +10)	138	0.0893	0.0126	0.0048	0.3663	<0.0001
	Right caudate	(+12 +10 +14)	95	0.2618	0.0375	0.0155	0.4975	<0.0001
	Right middle frontal gyrus	(+38 +20 +44)	90	0.2965	0.0401	0.0180	0.2781	<0.0001
DMN seed of RCrus I Anti-Correlations	Right superior parietal lobule	(+16 -62 +50)	8388	<0.0001	<0.0001	<0.0001	0.0033	<0.0001
	Right insula	(+38 +16 -02)	4011	<0.0001	<0.0001	<0.0001	0.0006	<0.0001
	Right supplementary motor area	(+04 +10 +52)	2131	<0.0001	<0.0001	<0.0001	0.0002	<0.0001
	Right middle frontal gyrus	(+36 +02 +70)	730	<0.0001	<0.0001	<0.0001	0.0036	<0.0001
	Left middle frontal gyrus	(-48 +34 +30)	411	0.0003	0.0001	<0.0001	0.8327	<0.0001
	Right parahippocampal gyrus	(+12 +06 -32)	352	0.0009	0.0002	<0.0001	0.0020	<0.0001
	Left lobule VIIIA/VIIB	(-40 -44 -54)	125	0.1232	0.0288	0.0067	0.2834	<0.0001
	Right middle orbitofrontal cortex	(-26 +36 -14)	110	0.1795	0.0379	0.0101	0.8097	<0.0001
FP seed of RCrus I Correlations	Right Crus I	(+38 -72 -28)	14391	<0.0001	<0.0001	<0.0001	<0.0001	<0.0001
	Left precentral gyrus/inferior frontal gyrus/middle frontal gyrus	(-36 +04 +36)	6339	<0.0001	<0.0001	<0.0001	<0.0001	<0.0001
	Left inferior parietal lobe	(-40 -46 +40)	3062	<0.0001	<0.0001	<0.0001	<0.0001	<0.0001
	Right superior occipital gyrus/superior parietal lobe/angular gyrus	(+28 -72 +42)	725	<0.0001	<0.0001	<0.0001	0.4946	<0.0001
	Right inferior frontal gyrus	(+52 +40 +18)	437	0.0001	<0.0001	<0.0001	0.0090	<0.0001
	Right precentral gyrus/inferior frontal gyrus	(+50 +08 +32)	182	0.0273	0.0091	0.0014	0.6871	<0.0001
	Left globus pallidus	(-12 +02 +00)	163	0.0432	0.0124	0.0022	0.7556	<0.0001
	Right inferior orbitofrontal cortex	(+48 +52 -14)	157	0.0501	0.0126	0.0025	0.6618	<0.0001
	Right supplementary motor area/superior frontal gyrus	(-04 +22 +48)	146	0.0659	0.0149	0.0034	0.9916	0.0001
FP seed of RCrus I Anti-Correlations	Right anterior cingulate cortex	(+06 +44 +12)	839	<0.0001	<0.0001	<0.0001	0.0602	<0.0001
	Right middle temporal gyrus	(+62 -48 +16)	352	0.0007	0.0007	<0.0001	0.2356	<0.0001
	Right superior temporal pole	(+34 +20 -36)	257	0.0050	0.0034	0.0002	0.7820	<0.0001
	Right heschl's gyrus	(+54 -10 +08)	182	0.0273	0.0120	0.0014	0.5087	<0.0001
	Left rolandic operculum	(-48 -24 +16)	179	0.0293	0.0120	0.0015	0.9717	0.0001

Supplementary Table 2. Functional connectivity during tDCS (anodal > sham)

Seed	Location	Clusters (x,y,z)	size	cluster p-FWE	cluster p-FDR	cluster p-unc	peak p-FWE	peak p-unc
RCrus I	Left inferior parietal lobe	(-40 -28 +38)	531	2×10^{-4}	2×10^{-4}	2×10^{-5}	1×10^{-2}	1×10^{-7}
Left inferior parietal lobe (IPL)	Right Crus I/II	(+30 -84 -30)	891	2×10^{-6}	4×10^{-6}	1×10^{-5}	9×10^{-3}	1×10^{-5}
	Left Crus I/II	(-12 -86 -32)	539	2×10^{-4}	2×10^{-4}	1×10^{-5}	0.2442	5×10^{-6}
	Left Superior frontal gyrus	(-20 +44 +54)	315	5×10^{-3}	3×10^{-3}	3×10^{-4}	0.56614	2×10^{-5}

Supplementary Table 3. Structural connectivity in mice

Interaction p-values							
		MPAC	MPAC-R	MPAC-L	LPAC	LPAC-R	LPAC-L
Lobule	Crus I (Full)	0.41	x	x	0.61	x	x
	Crus I Right	0.36	0.44	0.32	0.39	0.48	0.36
	Crus I Left	0.54	0.77	0.37	0.89	0.86	0.71
WM	Crus I (Full)	0.04	x	x	0.1	x	x
	Crus I Right	0.03	0.07	0.04	0.053	0.14	0.03
	Crus I Left	0.08	0.12	0.11	0.23	0.38	0.19
Both	Crus I (Full)	0.34	x	x	0.53	x	x
	Crus I Right	0.29	0.38	0.26	0.33	0.43	0.3
	Crus I Left	0.47	0.68	0.33	0.8	0.94	0.64
Correlation Coefficients (R) – Control							
		MPAC	MPAC-R	MPAC-L	LPAC	LPAC-R	LPAC-L
Lobule	Crus I (Full)	-0.13	x	x	-0.06	x	x
	Crus I Right	-0.2	-0.1	-0.28	-0.17	-0.09	-0.22
	Crus I Left	-0.05	0.08	-0.19	0.04	0.18	-0.07
WM	Crus I (Full)	-0.41	x	x	-0.3	x	x
	Crus I Right	-0.38	-0.3	-0.41	-0.33	-0.22	-0.38
	Crus I Left	-0.36	-0.33	-0.34	-0.23	-0.14	-0.28
Both	Crus I (Full)	-0.16	x	x	-0.09	x	x
	Crus I Right	-0.22	-0.12	-0.28	-0.16	-0.11	-0.24
	Crus I Left	-0.08	0.05	-0.21	0.02	0.16	-0.09
Correlation – p-value – Control							
		MPAC	MPAC-R	MPAC-L	LPAC	LPAC-R	LPAC-L
Lobule	Crus I (Full)	0.64	x	x	0.82	x	x
	Crus I Right	0.47	0.72	0.32	0.54	0.74	0.42
	Crus I Left	0.85	0.77	0.5	0.88	0.51	0.8
WM	Crus I (Full)	0.13	x	x	0.27	x	x
	Crus I Right	0.16	0.28	0.13	0.23	0.43	0.16
	Crus I Left	0.19	0.23	0.22	0.41	0.62	0.31
Both	Crus I (Full)	0.76	x	x	0.56	x	x
	Crus I Right	0.42	0.66	0.29	0.49	0.7	0.38
	Crus I Left	0.77	0.87	0.46	0.95	0.58	0.75
Correlation Coefficients (R) – Mutant							
		MPAC	MPAC-R	MPAC-L	LPAC	LPAC-R	LPAC-L
Lobule	Crus I (Full)	0.2	x	x	0.15	x	x
	Crus I Right	0.17	0.21	0.1	0.17	0.2	0.14
	Crus I Left	0.2	0.2	0.17	0.11	0.13	0.08

WM	Crus I (Full)	0.41	x	x	0.35	x	x
	Crus I Right	0.46	0.43	0.4	0.44	0.38	0.45
	Crus I Left	0.34	0.29	0.32	0.25	0.21	0.26
Both	Crus I (Full)	0.22	x	x	0.17	x	x
	Crus I Right	0.2	0.23	0.13	0.2	0.22	0.17
	Crus I Left	0.22	0.21	0.19	0.12	0.14	0.1
Correlation – p-value – Mutant							
	MPAC	MPAC-R	MPAC-L	LPAC	LPAC-R	LPAC-L	MPAC
Lobule	Crus I (Full)	0.5	x	x	0.62	x	x
	Crus I Right	0.57	0.47	0.72	0.55	0.5	0.63
	Crus I Left	0.49	0.5	0.56	0.71	0.66	0.78
WM	Crus I (Full)	0.14	x	x	0.21	x	x
	Crus I Right	0.1	0.12	0.15	0.11	0.18	0.11
	Crus I Left	0.24	0.32	0.26	0.38	0.46	0.37
Both	Crus I (Full)	0.57	x	x	0.45	x	x
	Crus I Right	0.5	0.42	0.38	0.49	0.45	0.56
	Crus I Left	0.46	0.47	0.52	0.67	0.64	0.73

Supplementary Table 4. Demographics of ASD and TD participants

Distribution of Participants	ASD	TD	X^2	p-value
Total number of participants	n=81	n=81	n/a	n/a
Male/female	64/17	65/16	0.65	0.72
Handedness: Right/Mixed/Left	68/4/9	68/6/7	0.65	0.72
Receiving coil: 8-/32-channel	55/26	57/24	0.03	0.86
Scan length: 128/156 volumes	65/16	68/13	0.17	0.68
Averages	**ASD**	**TD**	**t-value**	**p-value**
Age	10.36±1.44	10.39±1.17	-0.13	0.89
Socioeconomic status	52.9±10.1	50.1±10.8	1.5	0.14
General ability index	108.7±15.67	110.3±11.97	-0.72	0.47
Mean framewise displacement (mm)	0.37±0.25	0.33±0.26	1	0.31
ADOS Total	14.11±3.88	n/a	n/a	n/a
ADOS Social Interaction & Communication Total	11.42±3.39	n/a	n/a	n/a
ADOS RRB	2.7±1.73	n/a	n/a	n/a
ADI-R Reciprocal Social Interaction Total	20.2±5.5	n/a	n/a	n/a
ADI-R Communication Total	15.8±4.5	n/a	n/a	n/a
ADI-R RRS Behaviors Total	6.07±2.04	n/a	n/a	n/a

Supplementary Table 5. Behavioral tests in DREADD mice

Behavioral Test	n	p-value	F
SOCIAL APPROACH (novel animal vs. novel object)			
Time in Chamber		Bonferroni post-hoc comparisons	Two-way ANOVA F (2, 258) = 186.7
Control (GFP/RCrusI) VEH	12	**<0.0001**	
Control (GFP/RCrusI) CNO	10	**<0.0001**	
Control (LCrusI) CNO	10	**0.0001**	
Control (RCrusI) VEH	23	**0.0025**	
Control (RCrusI) CNO	22	0.0975	
Control (RCrusI, new) VEH	9	**0.0008**	
Control (RCrusI, new) CNO	9	>0.9999	
Time spent in Chamber with Novel Animal		Bonferroni post-hoc comparisons	Two-way ANOVA F (6, 264) = 0.02367
GFP: VEH vs. CNO		>0.999	
GFP (VEH) vs. RCrusI (CNO)		**0.0057**	
GFP (CNO) vs. RCrusI (CNO)		**0.0035**	
L CrusI (CNO) vs. RCrusI (CNO)		**0.0014**	
RCrusI: VEH vs. CNO		0.3215	
RCrusI (new): VEH vs. CNO		>0.999	
Time sniffing: Novel animal vs. novel object		Bonferroni post-hoc comparisons	Two-way ANOVA F (1, 174) = 95.96
Control (GFP/RCrusI) VEH		**<0.0001**	
Control (GFP/RCrusI) CNO		**<0.0001**	

Control (LCrusI) CNO		**<0.0001**	
Control (RCrusI) VEH		**<0.0001**	
Control (RCrusI) CNO		>0.9999	
Control (RCrusI, new) VEH		**0.0013**	
Control (RCrusI, new) CNO		>0.9999	
Time sniffing: Novel animal		Bonferroni post-hoc comparisons	Two-way ANOVA F (6, 174) = 3.915
GFP: VEH vs. CNO		>0.9999	
GFP (VEH) vs. RCrusI (CNO)		**<0.0001**	
GFP (CNO) vs. RCrusI (CNO)		**<0.0001**	
LCrusI (CNO) vs. RCrusI (CNO)		**<0.0001**	
RCrusI: VEH vs. CNO		**<0.0001**	
RCrusI (new): VEH vs. CNO		**0.043**	
Crossings		Bonferroni post-hoc comparisons	Two-way ANOVA F (4, 115) = 4.974
Control (GFP/RCrusI) VEH		0.3674	
Control (GFP/RCrusI) CNO		>0.9999	
Control (LCrusI) CNO		>0.9999	
Control (RCrusI) VEH		>0.9999	
Control (RCrusI) CNO		>0.9999	
SOCIAL NOVELTY			
Time in Chamber: Novel animal vs. novel object		Bonferroni post-hoc comparisons	Two-way ANOVA F (2, 258) = 274
Control (GFP/RCrusI) VEH	12	**<0.0001**	
Control (GFP/RCrusI) CNO	10	**0.0044**	

Control (LCrusI) CNO	10	**0.0002**	
Control (RCrusI) VEH	23	**<0.0001**	
Control (RCrusI) CNO	22	>0.9999	
Control (RCrusI, new) VEH	9	**0.0013**	
Control (RCrusI, new) CNO	9	0.0886	
Time spent in Chamber with Novel Animal		Bonferroni post-hoc comparisons	Two-way ANOVA F (6, 264) = 0.04315
GFP: VEH vs. CNO		>0.9999	
GFP (VEH) vs. RCrusI (CNO)		0.2014	
GFP (CNO) vs. RCrusI (CNO)		>0.9999	
LCrusI (CNO) vs. RCrusI (CNO)		0.1843	
RCrusI: VEH vs. CNO		**0.0132**	
RCrusI (new): VEH vs. CNO		>0.9999	
Time sniffing: Novel animal vs. Familiar animal		Bonferroni post-hoc comparisons	Two-way ANOVA F (1, 178) = 59.46
Control (GFP/RCrusI) VEH		**<0.0001**	
Control (GFP/RCrusI) CNO		**<0.0001**	
Control (LCrusI) CNO		**<0.0001**	
Control (RCrusI) VEH		**<0.0001**	
Control (RCrusI) CNO		>0.9999	
Control (RCrusI, new) VEH		**0.0013**	
Control (RCrusI, new) CNO		>0.9999	
Time sniffing: Novel animal		Bonferroni post-hoc comparisons	Two-way ANOVA F (6, 178) = 1.734
GFP: VEH vs. CNO		>0.9999	

GFP (VEH) vs. RCrusI (CNO)		**<0.0001**	
GFP (CNO) vs. RCrusI (CNO)		**<0.0001**	
LCrusI (CNO) vs. RCrusI (CNO)		**<0.0001**	
RCrusI: VEH vs. CNO		**<0.0001**	
RCrusI (new): VEH vs. CNO		**0.0430**	
Crossings		Bonferroni post-hoc comparisons	Two-way ANOVA F (4, 116) = 3.552
Control (GFP/RCrusI) VEH		>0.9999	
Control (GFP/RCrusI) CNO		>0.9999	
Control (LCrusI) CNO		>0.9999	
Control (RCrusI) VEH		>0.9999	
Control (RCrusI) CNO		>0.9999	
WATER T MAZE			
Control (GFP/RCrusI) VEH	12		
Control (GFP/RCrusI) CNO	9		
Control (LCrusI) CNO	12		
Control (RCrusI) VEH	12		
Control (RCrusI) CNO	12		
No. of Correct Responses		Bonferroni post-hoc comparisons	Two-way ANOVA F (4, 318) = 6.003
Trial 1-3		Trial 1/2/3	
RCrusI (GFP/VEH) vs. RCrusI (CNO)		>0.9999/>0.9999/0.7439	
RCrusI (GFP/CNO) vs. L CrusI (CNO)		>0.9999/>0.9999/>0.999	
RCrusI (GFP/CNO) vs. RCrusI (VEH)		0.4137/>0.9999/>0.9999	

RCrusI (GFP/CNO) vs. RCrusI (CNO)	>0.9999/>0.9999/>0.999	
L CrusI (CNO) vs. R CrusI (CNO)	>0.9999/>0.9999/>0.999	
R CrusI: VEH vs. CNO	>0.9999/>0.9999/>0.999	
Reversal Trial 1-3	Reversal Trial 1/2/3	
RCrusI (GFP/VEH) vs. RCrusI (CNO)	**0.0005/**0.0763/ >0.9999	
RCrusI (GFP/CNO) vs. LCrusI (CNO)	0.0536/>0.9999/>0.9999	
RCrusI (GFP/CNO) vs. RCrusI (VEH)	>0.9999/>0.9999/>0.999	
RCrusI (GFP/CNO) vs. RCrusI (CNO)	**<0.0001**/0.8013/>0.9999	
LCrusI (CNO) vs. RCrusI (CNO)	0.0763**/**0.0763/>0.9999	
RCrusI: VEH vs. CNO	**<0.0001/0.0351**/>0.9999	
No. of Trials prior to 5 Consecutive Correct Responses	Bonferroni post-hoc comparisons	Two-way ANOVA F (4, 318) = 5.408
Trial 1-3	Trial 1/2/3	
RCrusI (GFP/VEH) vs. RCrusI (CNO)	>0.9999/>0.9999/>0.999	
RCrusI (GFP/CNO) vs. LCrusI (CNO)	>0.9999/>0.9999/>0.999	
RCrusI (GFP/CNO) vs. RCrusI (VEH)	0.0727/>0.9999/>0.9999	
RCrusI (GFP/CNO) vs. RCrusI (CNO)	>0.9999/>0.9999/>0.999	
LCrusI (CNO) vs. RCrusI (CNO)	>0.9999/>0.9999/>0.999	
RCrusI: VEH vs. CNO	>0.9999/>0.9999/>0.999	
Reversal Trial 1-3	Reversal Trial 1/2/3	

RCrusI (GFP/VEH) vs. RCrusI (CNO)		**<0.0001/0.0296/**>0.9999	
RCrusI (GFP/CNO) vs. LCrusI (CNO)		0.5414**/**>0.9999**/**>0.9999	
RCrusI (GFP/CNO) vs. RCrusI (VEH)		>0.9999**/**>0.9999**/**>0.9999	
RCrusI (GFP/CNO) vs. RCrusI (CNO)		**<0.0001/**0.056**/**>0.9999	
LCrusI (CNO) vs. RCrusI (CNO)		**0.0139/0.0296/**>0.9999	
RCrusI: VEH vs. CNO		**<0.0001/0.0027/**>0.9999	
GROOMING			
Control (GFP/RCrusI) VEH	12		
Control (GFP/RCrusI) CNO	10		
Control (LCrusI) CNO	12		
Control (RCrusI) VEH	27		
Control (RCrusI) CNO	29		
Control RCrusI (new) VEH	8		
Control RCrusI (new) CNO	8		
		Bonferroni post-hoc comparisons	One-way ANOVA F (6, 110) = 9.562
RCrusI (GFP/VEH) vs. RCrusI (CNO)		**0.0039**	
RCrusI (GFP/CNO) vs. LCrusI (CNO)		0.9768	
RCrusI (GFP/CNO) vs. RCrusI (VEH)		0.9996	
RCrusI (GFP/CNO) vs. RCrusI (CNO)		**0.0071**	
LCrusI (CNO) vs. RCrusI (CNO)		0.0830	
RCrusI: VEH vs. CNO		**<0.0001**	
RCrusI (new): VEH vs. CNO		**0.0009**	

ROTAROD			
Control (GFP/RCrusI) VEH	14		
Control (GFP/RCrusI) CNO	12		
Control (LCrusI) CNO	9		
Control (RCrusI) VEH	10		
Control (RCrusI) CNO	10		
		Bonferroni post-hoc comparisons	Two-way ANOVA F (4, 234) = 0.8734
RCrusI (GFP/VEH) vs. RCrusI (CNO)		>0.9999	
RCrusI (GFP/CNO) vs. LCrusI (CNO)		>0.9999	
RCrusI (GFP/CNO) vs. RCrusI (VEH)		>0.9999	
RCrusI (GFP/CNO) vs. RCrusI (CNO)		>0.9999.	
LCrusI (CNO) vs. RCrusI (CNO)		>0.9999	
RCrusI: VEH vs. CNO		>0.9999	
OPEN FIELD			
Control (GFP/RCrusI) VEH	12		
Control (GFP/RCrusI) CNO	12		
Control (LCrusI) CNO	12		
Control (RCrusI) VEH	36		
Control (RCrusI) CNO	25		
Distance*		Bonferroni post-hoc comparisons	Two-way ANOVA F (4, 1380) = 51.49
RCrusI (GFP/VEH) vs. RCrusI (CNO)		>0.9999	

RCrusI (GFP, CNO) vs. LCrusI (CNO)		**0.0007**	
RCrusI: (GFP/CNO) vs. (VEH)		>0.9999	
RCrusI: (GFP/CNO) vs. (CNO)		>0.9999	
LCrusI (CNO) vs. RCrusI (CNO)		**<0.0001**	
RCrusI: (VEH) vs. (CNO)		>0.9999	
• ***Pvalues for 0-1 min time bin. For non-significant values: no significant differences in any time bin 0-15 min. For LCrusI, significant differences in first three time bins (0-3 min).***			
Center Time		Bonferroni post-hoc comparisons	One-way ANOVA F (4,92) = 2.752
RCrusI (GFP, VEH) vs. RCrusI (CNO)		>0.9999	
RCrusI (GFP, CNO) vs. LCrusI (CNO)		0.0582	
RCrusI: (GFP/CNO) vs. (VEH)		>0.9999	
RCrusI: (GFP/CNO) vs. (CNO)		>0.9999	
LCrusI (CNO) vs. RCrusI (CNO)		0.2147	
RCrusI: (VEH) vs. (CNO)		>0.9999	
ELEVATED PLUS MAZE			
Control (GFP/RCrusI) VEH	12		
Control (GFP/RCrusI) CNO	12		
Control (LCrusI) CNO	13		
Control (RCrusI) VEH	22		
Control (RCrusI) CNO	17		
Distance		Bonferroni post-hoc comparisons	One-way ANOVA

		F (4, 78) = 1.815
RCrusI (GFP, VEH) vs. RCrusI (CNO)	0.7580	
RCrusI (GFP, CNO) vs. LCrusI (CNO)	>0.9999	
RCrusI: (GFP/CNO) vs. (VEH)	>0.9999	
RCrusI: (GFP/CNO) vs. (CNO)	0.2796	
LCrusI (CNO) vs. RCrusI (CNO)	0.2493	
RCrusI: (VEH) vs. (CNO)	0.1683	
Open Arm (time)	Bonferroni post-hoc comparisons	One-way ANOVA F (4, 77) = 1.315
RCrusI (GFP, VEH) vs. RCrusI (CNO)	0.2651	
RCrusI (GFP, CNO) vs. LCrusI (CNO)	0.9460	
RCrusI: (GFP/CNO) vs. (VEH)	0.9998	
RCrusI: (GFP/CNO) vs. (CNO)	0.7165	
LCrusI (CNO) vs. RCrusI (CNO)	0.9887	
RCrusI: (VEH) vs. (CNO)	0.4708	
OLFACTION	Bonferroni post-hoc comparisons	Two-way ANOVA F (1,240) = 3.049
RCrusI: (VEH) vs. (CNO): social olfactory cues. *All non social olfactory cues: p >0.9999	A: **<0.0001**/>0.99/>0.99 B: **0.0206**/>0.99/>0.99	
LIGHT/DARK BOX		

Light vs. Dark	Bonferroni post-hoc comparisons	Two-way ANOVA F(1,64) = 162.7
RCrusI GFP (VEH)	**<0.0001**	
RCrusI GFP (CNO)	**0.0001**	
RCrusI (VEH)	**<0.0001**	
RCrusI (CNO)	**<0.0001**	
RHYTHMIC LICKING		
Lick Duration	Unpaired t-test	
RCrusI: VEH vs. CNO	0.4265	
Inter – lick interval		
RCrusI: VEH vs. CNO	0.7404	

Supplementary Table 6. Behavioral tests in mutant mice

Behavioral Test	n	p-value	F
SOCIAL APPROACH			
Time in Chamber: Novel animal vs. novel object		Bonferroni post-hoc comparisons	Two-way ANOVA F (2, 174) = 162.2
Mutant: GFP (VEH)	17	0.5938	
Mutant: GFP (CNO)	10	0.9174	
Mutant: LCrusI (CNO)	11	>0.9999	
Mutant: RCrusI (VEH)	13	0.9392	
Mutant: RCrusI (CNO)	14	**<0.0001**	
Time spent in Chamber with Novel Animal		Bonferroni post-hoc comparisons	Two-way ANOVA F (4, 174) = 0.002819
Mutant: GFP (VEH) vs. (CNO)		>0.9999	
Mutant: GFP (VEH) vs. RCrusI (CNO)		0.4555	
Mutant: GFP (CNO) vs. RCrusI CNO		>0.9999	
Mutant: LCrusI (CNO) vs. RCrusI (CNO)		0.3976	
Mutant: RCrusI (VEH) vs. (CNO)		0.3668	
Time sniffing: Novel animal vs. novel object		Bonferroni post-hoc comparisons	Two-way ANOVA F (11, 120) = 12.15
Mutant: GFP (VEH)		>0.9999	
Mutant: GFP (CNO)		>0.9999	
Mutant: LCrusI (CNO)		>0.9999	
Mutant: RCrusI (VEH)		>0.9999	
Mutant: RCrusI (CNO)		**<0.0001**	
Time sniffing: novel animal		Bonferroni post-hoc comparisons	Two-way ANOVA F (4, 120) = 6.899
Mutant: GFP (VEH) vs. GFP (CNO)		0.3645	
Mutant: GFP (VEH) vs. RCrusI (CNO)		**<0.0001**	
Mutant: GFP (CNO) vs. RCrusI CNO		**0.0021**	

Mutant: LCrusI (CNO) vs. RCrusI (CNO)		**<0.0001**	
Mutant: RCrusI (VEH) vs. (CNO)		**<0.0001**	

SOCIAL NOVELTY

Time in Chamber: Novel animal vs. novel object		Bonferroni post-hoc comparisons	Two-way ANOVA F (2, 174) = 104.3
Mutant: GFP (VEH)	17	>0.9999	
Mutant: GFP (CNO)	10	>0.9999	
Mutant: LCrusI (CNO)	11	>0.9999	
Mutant: RCrusI (VEH)	14	>0.9999	
Mutant: RCrusI (CNO)	15	**0.0007**	

Time spent in Chamber with Novel Animal	Bonferroni post-hoc comparisons	Two-way ANOVA F (4, 174) = 0.02577
Mutant: GFP (VEH) vs. GFP (CNO)	>0.9999	
Mutant: GFP (VEH) vs. RCrusI (CNO)	0.6949	
Mutant: GFP (CNO) vs. RCrusI CNO	0.3160	
Mutant: LCrusI (CNO) vs. RCrusI (CNO)	>0.9999	
Mutant: RCrusI (VEH) vs. (CNO)	>0.9999	

Time sniffing: Novel animal vs. novel object	Bonferroni post-hoc comparisons	Two-way ANOVA F (1, 120) = 7.11
Mutant: GFP (VEH)	>0.9999	
Mutant: GFP (CNO)	>0.9999	
Mutant: LCrusI (CNO)	>0.9999	
Mutant: RCrusI (VEH)	>0.9999	
Mutant: RCrusI (CNO)	**<0.0001**	

Time spent in Chamber with Novel Animal	Bonferroni post-hoc comparisons	Two-way ANOVA F (4, 120) = 2.466
Mutant: GFP (VEH) vs. GFP (CNO)	n.s.	
Mutant: GFP (VEH) vs. RCrusI (CNO)	**0.0012**	

Mutant: GFP (CNO) vs. RCrusI CNO	0.0776
Mutant: LCrusI (CNO) vs. RCrusI (CNO)	**0.0007**
Mutant: RCrusI (VEH) vs. (CNO)	**0.0076**

WATER T MAZE

Mutant GFP (VEH)	9
Mutant GFP (CNO)	10
Mutant LCrusI (CNO)	7
Mutant RCrusI (VEH)	7
Mutant RCrusI (CNO)	8

No. of Correct Responses	Bonferroni post-hoc comparisons	Two-way ANOVA F (4, 216) = 1.257
Trial 1-3	Trial 1/2/3	
Mutant: GFP (VEH) vs. GFP (CNO)	>0.999/>0.999/>0.999	
Mutant: GFP (VEH) vs. RCrusI (CNO)	>0.999/>0.999/>0.999	
Mutant: GFP (CNO) vs. RCrusI CNO	>0.999/>0.999/>0.999	
Mutant: LCrusI (CNO) vs. RCrusI (CNO)	>0.999/>0.999/>0.999	
Mutant: RCrusI (VEH) vs. (CNO)	>0.999/>0.999/>0.999	
Reversal Trial 1-3	Reversal Trial 1/2/3	
Mutant: GFP (VEH) vs. GFP (CNO)	>0.999/0.5363/>0.999	
Mutant: GFP (VEH) vs. RCrusI (CNO)	>0.999/0.4558/>0.999	
Mutant: GFP (CNO) vs. RCrusI CNO	>0.999/>0.999/>0.999	
Mutant: LCrusI (CNO) vs. RCrusI (CNO)	>0.999/>0.999/>0.999	
Mutant: RCrusI (VEH) vs. (CNO)	>0.999/>0.999/>0.999	

No. of Trials prior to 5 Consecutive Correct Responses	Bonferroni post-hoc comparisons	Two-way ANOVA F (4, 216) = 1.466
Trial 1-3	Trial 1/2/3	
Mutant: GFP (VEH) vs. GFP (CNO)	>0.999/>0.999/>0.999	

Mutant: GFP (VEH) vs. RCrusI (CNO)		>0.999/>0.999/>0.999	
Mutant: GFP (CNO) vs. RCrusI CNO		>0.999/>0.999/>0.999	
Mutant: LCrusI (CNO) vs. RCrusI (CNO)		>0.999/>0.999/>0.999	
Mutant: RCrusI (VEH) vs. (CNO)		>0.999/>0.999/>0.999	
Reversal Trial 1-3		Reversal Trial 1/2/3	
Mutant: GFP (VEH) vs. GFP (CNO)		>0.999/>0.999/>0.999	
Mutant: GFP (VEH) vs. RCrusI (CNO)		>0.999/0.1440/>0.999	
Mutant: GFP (CNO) vs. RCrusI CNO		>0.999/0.4813/>0.999	
Mutant: LCrusI (CNO) vs. RCrusI (CNO)		>0.999/>0.999/>0.999	
Mutant: RCrusI (VEH) vs. (CNO)		>0.999/>0.999/>0.999	
GROOMING			
Mutant GFP (VEH)	13		
Mutant GFP (CNO)	10		
Mutant LCrusI (CNO)	11		
Mutant RCrusI (VEH)	14		
Mutant RCrusI (CNO)	12		
		Bonferroni post-hoc comparisons	One-way ANOVA F (4, 57) = 0.9732
Mutant: GFP (VEH) vs. GFP (CNO)		>0.9999	
Mutant: GFP (VEH) vs. RCrusI (CNO)		>0.9999	
Mutant: GFP (CNO) vs. RCrusI CNO		>0.9999	
Mutant: LCrusI (CNO) vs. RCrusI (CNO)		>0.9999	
Mutant: RCrusI (VEH) vs. (CNO)		>0.9999	
ROTAROD			
Mutant GFP (VEH)	9		
Mutant GFP (CNO)	10		
Mutant LCrusI (CNO)	11		

Mutant RCrusI (VEH)	8		
Mutant RCrusI (CNO)	7		
		Bonferroni post-hoc comparisons	Two-way ANOVA F (4, 190) = 1.167
Mutant: GFP (VEH) vs. GFP (CNO)		>0.9999	
Mutant: GFP (VEH) vs. RCrusI (CNO)		>0.9999	
Mutant: GFP (CNO) vs. RCrusI CNO		>0.9999	
Mutant: LCrusI (CNO) vs. RCrusI (CNO)		>0.9999	
Mutant: RCrusI (VEH) vs. (CNO)		>0.9999	
OPEN FIELD			
Mutant GFP (VEH)	14		
Mutant GFP (CNO)	10		
Mutant LCrusI (CNO)	11		
Mutant RCrusI (VEH)	15		
Mutant RCrusI (CNO)	15		
Distance		Bonferroni post-hoc comparisons	Two-way ANOVA F (2, 549) = 22.14
Mutant: GFP (VEH) vs. GFP (CNO)		>0.9999	
Mutant: GFP (VEH) vs. RCrusI (CNO)		0.7208	
Mutant: GFP (CNO) vs. RCrusI CNO		>0.9999	
Mutant: LCrusI (CNO) vs. RCrusI (CNO)		**0.0019**	
Mutant: RCrusI (VEH) vs. (CNO)		>0.9999	
*pvalues shown from time bin 0-1 min. No significant differences were detected within any additional time bins for all comparisons tested.			
Center Time		Bonferroni post-hoc comparisons	One-way ANOVA F (4, 55) = 0.7183
Mutant: GFP (VEH) vs. GFP (CNO)		>0.9999	
Mutant: GFP (VEH) vs. RCrusI (CNO)		>0.9999	

Mutant: GFP (CNO) vs. RCrusI CNO		>0.9999	
Mutant: LCrusI (CNO) vs. RCrusI (CNO)		>0.9999	
Mutant: RCrusI (VEH) vs. (CNO)		>0.9999	

ELEVATED PLUS MAZE

Mutant GFP (VEH)	16
Mutant GFP (CNO)	10
Mutant LCrusI (CNO)	11
Mutant RCrusI (VEH)	15
Mutant RCrusI (CNO)	15

Open Arms	Bonferroni post-hoc comparisons	One-way ANOVA F (4, 62) = 1.608
Mutant: GFP (VEH) vs. GFP (CNO)	0.9940	
Mutant: GFP (VEH) vs. RCrusI (CNO)	>0.9999	
Mutant: GFP (CNO) vs. RCrusI CNO	0.9622	
Mutant: LCrusI (CNO) vs. RCrusI (CNO)	0.9999	
Mutant: RCrusI (VEH) vs. (CNO)	0.5388	

Distance	Bonferroni post-hoc comparisons	One-way ANOVA F (4, 62) = 1.332
Mutant: GFP (VEH) vs. GFP (CNO)	>0.9999	
Mutant: GFP (VEH) vs. RCrusI (CNO)	>0.9999	
Mutant: GFP (CNO) vs. RCrusI CNO	>0.9999	
Mutant: LCrusI (CNO) vs. RCrusI (CNO)	>0.9999	
Mutant: RCrusI (VEH) vs. (CNO)	0.3084	

Supplementary Data

tDCS symptom checklists. Following the scanning session, participants completed a 26-item self-scored questionnaire to rate the occurrence and intensity of side effects during and after tDCS such as tingling, burning, itching, fatigue, pain, etc.. Participants rated the extent to which they experienced these symptoms on a continuous scale of 1 (not at all) to 10 (greatest imaginable). Between-group (sham vs. anodal) symptom differences were analyzed using two-sample t-tests. The highest scores were given for "tingling" (anodal $\mu=3.8\pm2.73$; sham $\mu=2.5\pm2.17$) and "burning" (anodal $\mu=2.6\pm2.81$; sham $\mu=1.1\pm1.73$). There were no between-group differences between these symptoms (tingling $p=0.12$; burning $p=0.08$, two-sample t-tests), or on any of the other items on the symptom questionnaire (all p values>0.05).